Density Functional Theory (DFT) studies on extraction of Europium and Americium from Spent Nuclear Waste

By

Nimra Khan

NUST00000326111

Supervisor

Dr. Uzma Habib

MS Computational Science and Engineering

School of Interdisciplinary Engineering and Sciences

National University of Sciences and Technology

Islamabad, Pakistan

2022

Density Functional Theory (DFT) studies on extraction of Europium and Americium from Spent Nuclear Waste

By

Nimra Khan

NUST00000326111

Supervisor

Dr. Uzma Habib

MS Computational Science and Engineering

School of Interdisciplinary Engineering and Sciences

National University of Sciences and Technology

Islamabad, Pakistan

2022

Annex A to NUST Letter No. 0972/102/Exams/Thesis-Cert dated 23 Dec 16.

THESIS ACCEPTANCE CERTIFICATE

Certified that final copy of MS/MPhil thesis written by Ms**. Nimra Khan**, Registration No. **NUST2020326111** of **SINES** has been vetted by the undersigned, found complete in all aspects as per NUST Statutes/Regulations, is free of plagiarism, errors, and mistakes, and is accepted as partial fulfillment for the award of MS/MPhil degree. It is further certified that necessary amendments as pointed out by GEC members of the scholar have also been incorporated in the said thesis.

Signature with stamp: _____

Name of Supervisor: Dr. Uzma Habib
Date: _____

Signature of HoD with stamp: _____
Date: _____

Countersign by

Signature (Dean/Principal): _____
Date: _____

DECLARATION

I hereby declare that my thesis work, titled **—** ***Density Functional Theory (DFT) studies on extraction of Europium and Americium from Spent Nuclear Waste***, is carried out by me under the supervision of Dr. Uzma Habib at School of interdisciplinary Engineering and Science (SINES) in National University of Sciences and Technology (NUST). I solemnly declare that to the best of my knowledge, this is my original work, and it contains no material which has been accepted for the award of other degrees in my name, in any other university. Also, no material previously published or written by any other person has been included in this thesis except where due reference has been made to the previously published work.

Nimra Khan

MS Computational Science & Engineering

STATEMENT OF ORIGINALITY

With this statement, I hereby declare that the submitted Master's thesis is, to the best of my knowledge, my own original work. I certify that the intellectual content of this thesis is the result of my own hard work and that all the assistance received in preparing this thesis and sources have been acknowledged.

Nimra Khan

Dedicated to my beloved parents and siblings, whose unwavering support and cooperation enabled me to accomplish this wonderful goal.

ACKNOWLEDGEMENTS

First of all, my heartily gratitude is to Almighty Allah for giving me the valor to complete this research project.

Secondly, I am extremely grateful and indebted to my research supervisor, Dr. Uzma Habib for her expert, valuable, and sincere guidance, and encouragement during this research. I owe my deepest gratitude to my GEC members, Dr. Ammar Mushtaq associate professor at school of interdisciplinary engineering and sciences (SINES), NUST and Dr. Mudassir Iqbal associate Professor at school of natural sciences (SNS), NUST, for their boundless support and guidance.

Last, but not the least, I would like to say a very special thanks to my friends and family, especially my affectionate parents and my siblings for their love, care, and support during the course of this project.

Nimra Khan

Table of Contents

List of Figures

List of Tables

List of abbreviations

Abstract

Spent nuclear waste produced by nuclear reactors containing several long-lived radioactive nuclei, including uranium, plutonium, Fission products, and minor actinides (Np, Am, Cm), is hazardous. Extraction of highly radioactive nuclides with longer half-lives, in particular minor actinides, is required for safe and long-term waste disposal. However, it is a very difficult and challenging step in the spent nuclear fuel reprocessing to separate trivalent actinides, particularly Am^{+3} from trivalent lanthanides i.e., Eu^{+3}, due to their similar physiochemical properties such as chemical nature, oxidation state, and ionic radii. In this work, Density Functional Theory (DFT) calculations at the energy level of B3LYP/SDD hybrid density functional were conducted to evaluate the extraction behavior of Am^{+3} and Eu^{+3} metal with the organo phosphinodithioic acid ligand and its derivatives in the ratios of 1:1, 1:2, and 1:3 in n-dodecane solvent. The obtained computational findings confirmed that a 1:2 metal-ligand ratio is the ideal ratio for extracting the Am/Eu metals in n-dodecane solvent using organo phosphinodithioic acid ligands. Moreover, it has been found that Am is best extracted with an organo phosphinodithioic acid ligand derivative, benzyl(phenyl) phosphinodithioic acid (BphPT2), whereas Eu is best extracted with pyridazin-3-yl(pyridazin-3-ylmethyl) phosphinodithioic acid (PPPT2).

1 Introduction

1.1 Europium/Americium

Europium, with the symbol Eu, atomic number (Z) 63, and atomic mass number (A) 151.964 u, was first discovered in Europe in 1901 and is named europium because of its origin. It is a member of the lanthanide series and belongs to the f-block, with an electronic configuration of [Xe] $4f^7$ $6s^2$ [1], [2]. Being an element of the lanthanide series, europium in most of its compounds shows +3 oxidation state, but the oxidation state of +2 is also frequent in other compounds. Because of the half-filled 4f orbital, Eu^{+2} oxidation state is anomalous as compared to the other lanthanides. This divalent europium has a reducing property and is oxidized in air and water to form compounds with Eu^{+3} oxidation state as Eu^{+3} is more stable than Eu^{+2} [3].

Europium is a highly reactive and rare element found in the earth's crust at a concentration of about 1 ppm. The major mineral sources for europium, which contain barely 0.1% or less of it are [2], [4]:

- Bastnasite
- Monazite
- Xenotime

Naturally, europium has two isotopes ^{151}Eu and ^{153}Eu. ^{153}Eu is the most abundant with 52% natural abundance and is stable, whereas ^{151}E has a natural abundance of 48% and is unstable, undergoing alpha decay (in spontaneous fission of U) due to its unstable nature, with a half-life of 13-16 years [5].

Americium is an artificially synthesized chemical element with the symbol Am, atomic number (Z) 95, and atomic mass number (A) 243 u. It was first produced as a beta decay of plutonium upon bombardment of neutrons, in 1944 at the University of Chicago [6]. Americium being a member of f-block holds the mid-position of the actinide series with an electronic configuration of [Rn] $5f^7$ $7s^2$ [6], [7]. It can be found in a range of different oxidation states, including +3, +4, +5, +6, and +7, the most common and stable of which is Am+3, which is chemically similar to europium. By oxidizing the Am^{+3}, higher oxidation states of americium, greater than +3, can be obtained [8].

There are 13 isotopes of americium identified so far, with mass numbers ranging from 232 to 247 and half-lives ranging from 55 seconds to 7370 years [7], [8]. ^{241}Am, ^{242}Am, and ^{243}Am are the most common americium isotopes, with half-lives of 432, 143, and 7370 years, respectively [7], [9]. Between 1945 and 1980, americium was detected in the regions used for atmospheric nuclear weapons tests, as well as at the sites of nuclear disasters such as the Chernobyl disaster. Moreover, it is produced as a minor actinide byproduct of nuclear fuel cycle operations in nuclear power reactors [9].

Both europium and americium fractions are produced by neutron activation in nuclear processes. As some of the isotopes of europium and americium produced during the nuclear fuel cycle have long half-lives and high radiotoxicity, they are extremely dangerous to all living things and require safe disposal.

1.2 Nuclear Waste

It has been anticipated that global energy consumption will increase significantly in the next few years because of the world's fast-growing population and urbanization. Due to the depletion of fossil fuel resources and the need to minimize greenhouse gas emissions in the atmosphere, of which fossil fuel is one of the major contributors, a greater focus on "economical, green, and efficient" energy source is required at this time. As a result, nuclear power is emerging as the most viable choice for meeting global energy demand as it can produce a significant amount of energy while emitting no greenhouse gases and, more importantly, produces very little amount of waste [10], [11]. However, the generation of nuclear waste, which is harmful, restricts the use of nuclear power on a broad scale. This nuclear waste releases radioactive particles that last for thousands of years, posing long-term radiotoxicity risks to the environment and human health [10].

Nuclear waste refers to anything that is either naturally radioactive or has been contaminated by radioactivity. It consists of a number of radionuclides that are formed as a by-product of various nuclear reactions in nuclear power reactors, different steps of the nuclear fuel cycle and nuclear weapons development, as well as to a lesser extent from the research, agriculture, and medicine industries [12], [13].

Nuclear waste contains a mix of radionuclides with short and long half-lives, such as americium, europium, plutonium, uranium and many more. Each radioactive element has a half-life, which is the amount of time it takes for half of its atoms to decay and lose half of its

radioactivity. Long-lived radioactive elements emit less penetrating α and β-rays, whereas those with shorter half-lives emit γ-rays, which are more penetrating. All radioactive elements present in nuclear waste ultimately decay into nonradioactive elements, lowering the risk of nuclear waste, unlike other hazardous industrial wastes [14].

1.3 Classification of Nuclear Waste

Nuclear waste can be classified in a variety of ways, including chemical composition, aggregate state, mechanical properties, and so on, but the origin of the waste, radiological properties, and the type of radionuclides in the waste are the main characteristics. According to its source of origin and level of radioactivity, nuclear waste is usually divided into three categories: low-level waste, intermediate-level waste, and high-level waste [14], [15].

1.3.1 Low-Level Waste (LLW)

Low-Level Waste (LLW) comprises short-lived radionuclides and is responsible for a small amount of radioactivity but is considerably above clearance levels, which can be handled easily with minimal precautions.

LLW comes from many sources, including nuclear power plants, hospitals, and research institutions. It consists of radioactively contaminated filters, piping, containers, paper towels, lab coats, plastic, and paper products used in the nuclear fuel cycle at nuclear power plants and medical and research laboratories. This type of nuclear waste accounts for about 90% of the total waste volume but only 1% of the total emitted radioactivity [14], [16]. As LLW is non-heat generating and is safe to handle and transport, it can be simply disposed of in near-surface repositories (typically 30 m depth) [13].

1.3.2 Intermediate-Level Waste (ILW)

Compared to Low-Level Waste (LLW), the radioactivity of **Intermediate-Level Waste (ILW**) is much higher because it contains several long-lived fission products and alpha-emitting radionuclides that do not decay to a level of activity concentration suitable for near-surface disposal [15].

It usually consists of resins, chemical sludges, and contaminated materials produced during primary waste treatment and spent fuel reprocessing at nuclear power plants. ILW makes up to 7% of the total nuclear waste volume and accounts for about 4% of overall radioactivity. Because of the heat it produces (<2 kW/m^3) and higher amounts of radioactivity, this waste poses a significant risk to the environment if it is allowed to enter freely, and thus needs a greater degree of containment and shielding than LLW. It can be buried at depths ranging from tens of meters to a few hundred meters in subsurface repositories [14], [15].

1.3.3 High-Level Waste (HLW)

High-Level Waste (HLW) is a radiotoxic nuclear waste with a high concentration of both short and long-lived radionuclides, such as fission products and transuranic elements produced in the reactor core.

It is mainly generated by highly activated parts of the nuclear reactor and reprocessing of spent nuclear fuel. However, despite accounting for only 3% of total nuclear waste volume, it is responsible for 95% of all emitted radioactivity. Because HLW is a highly radioactive waste with a large amount of decay heat (> 2 kW/m^3), it necessitates a higher degree of containment and isolation for long-term safety. As a result, HLW must be properly shielded and cooled before being disposed of in deep, stable geological repositories, which are typically several hundred meters deep [14].

1.3.3.1 Spent Nuclear Fuel (SNF)

Spent Nuclear Fuel (SNF) is considered a form of HLW because it is highly radioactive used nuclear fuel that has been irradiated in all operating nuclear reactors and is no longer useful in generating electricity [14].

It contains a large number of fission products (FPs) which are the lighter elements produced by the asymmetric fission of heavier uranium and plutonium nuclei in a reactor, as well as a significant amount of transuranium (TRU) elements. These TRUs are heavier than uranium and are produced in a series of successive nuclear reactions by neutron capture of mainly ^{238}U [17], [18].

Generation of Transuranic elements

$$^{238}U_{92} + {}^{1}n_{0} \rightarrow {}^{239}U_{92} + \gamma \rightarrow {}^{239}Np_{93} + {}_{-1}\beta^{0} \rightarrow {}^{239}Pu_{94} + {}_{-1}\beta^{0}$$

$$^{239}Pu_{94} + {}^{1}n_{0} \rightarrow {}^{240}Am_{95} + {}_{-1}e^{0}$$

Fission products and minor actinides typically consist of $^{134,135,137}Cs$, ^{90}Sr, ^{99}Tc, $^{131,129}I$, $^{141,144}Pm$, ^{151}Sm, $^{152,154}Eu$ and ^{237}Np, $^{238,239}Pu$, $^{241,\ 243}Am$, $^{242,244}Cm$ respectively [19].

The composition, heat output and radioactivity per ton of heavy metal of the spent fuel depend upon the burn-up (burnup is a measure for the energy produced per mass of initial fuel in gigawatt-days/metric ton of heavy metal (GWd/Thm) [20]. For example, spent fuel with a burnup of 50 GWd/Thm consists of about 93.4% uranium, 1.2% plutonium, 5.2% fission products, and 0.2% minor transuranic elements (neptunium, americium, and curium) [21].

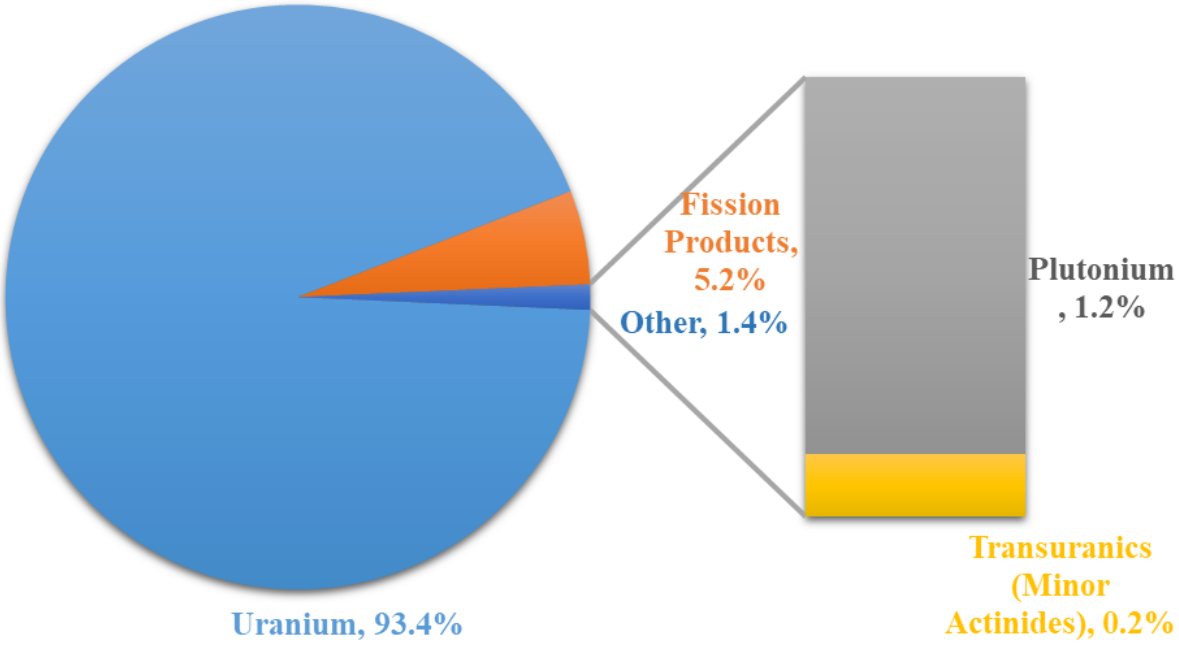

Figure 1.1 Spent fuel composition with a burnup of 50 GWd/Thm.

1.4 Need for Spent Fuel Management

The nuclear power industry, like all other industries, produces some waste. Even though the volume of waste created during the generation of nuclear energy is very little, a large portion of it is radioactive and must therefore be handled with extreme caution as a harmful material. Radionuclides are produced during the entire nuclear fuel cycle which gradually decompose into innocuous elements. Some radionuclides decay relatively slowly whereas others do so in hours or even minutes. The burning of nuclear fuel produces hundreds of radionuclides, most of which are very short-lived and decay to low levels in a matter of days to years, such as Lanthanum-140, Strontium-89, and Cerium-144, which have half-lives of 40 hours, 54 days, and 1.3 years, respectively. Hence for long-term disposal, the short-lived radionuclides generally do not pose a significant issue [22].

The problem of the long-lasting radiotoxic nature of the spent nuclear waste is because it holds long-lived ($\geq 10^3$-10^6 years) radioactive elements [23]. Despite their relatively small mass in spent fuel, transuranic elements, and some long-lived fission products are the primary contributors to long term radiotoxicity and long-term heat generation in spent fuel [24]. Fission product isotopes like Cesium-137, Iodine-129 and Technecium-99 with half-lives of 30 years, 1.7×10^7 years, and 2×10^6 years, respectively, are mostly responsible for the thermal heat from the fuel because they emit highly penetrating ionizing radiations (β and γ). Less penetrating radiations from α-decay events, on the other hand, mainly comes from very long-lived actinides, such as Americium-243, Plutonium-239, and Neptunium-237, with half-lives of 7300 years, 24000 years, and 2.1×10^6 years, respectively, but they decay much more slowly and pose long-term environmental risks [22], [25].

Thus, to avoid the long-term environmental damage, spent nuclear fuel requires adequate treatment, shielding, and, in certain conditions, further cooling. Because spent nuclear fuel emits heat and radiation as a result of radioactive decay and cannot be reprocessed or disposed of immediately, it is kept in special water pools on site for several years. Such pools are used for short-term cooling of spent fuel, as they allow short-lived isotopes to decay, reducing the heat and radioactivity [26].

Figure 1.2 Spent nuclear fuel pool, copied from https://www.oecd-nea.org/jcms/pl_47481/spent-nuclear-fuel-pool?details=true.

There are some specific methods proposed for the long-term management of spent fuel, including geological disposal, space disposal, reprocessing, and transmutation.

1.4.1 Deep Geological Disposal

Geological disposal usually involves burying of nuclear waste 500-1000 meters deep into the ground that is well away from the surface environment. The idea of deep geological disposal is based on a 'multi-barrier' system in which radioactive waste is protected from the environment by a combination of manmade and natural barriers (host rock). Nuclear waste containers (e.g., carbon steel, stainless steel, copper iron alloy), waste containers surrounded by a buffer backfill material (e.g., bentonite and concrete buffers/backfill), engineered repository, and the geological environment (e.g., geology, hydrogeology) all act as barriers to radionuclide release and transport in this multiple barrier system [27], [28].

1.4.2 Space Disposal

Space disposal implies loading of nuclear waste onto a space shuttle and launching the shuttle into the space. From a technical standpoint, this appears to be practical for a small amount of nuclear waste. However, because of the high launch rate needed, as well as the associated environmental impact, energy requirements, and cost factors, disposing of all high-level nuclear waste in space is impracticable. Although space disposal has emerged an option for the long-term management of nuclear waste, but it is not a preferred choice [29].

1.4.3 Reprocessing

Reprocessing is a series of chemical operations that recover useable components of spent fuel. Spent fuel contains significant amounts of fissile elements, such as ^{235}U, ^{233}U, and plutonium which can be re-used as fresh fuel for present and future nuclear power plants as well as to build nuclear weapons. Uranium and plutonium recovery reduces the volume and level of radioactivity of the material to be disposed of as HLW. As a result, spent fuel reprocessing lowers the long-term risk to people and the environment. However, nuclear reprocessing as a method of managing spent fuel is a complicated matter that must take into account a variety of considerations, including safety, economics, sustainable development, non-proliferation, and the environment. [18], [30].

1.4.4 Partitioning and Transmutation

Since the release of the US National Research Council’s report, 'The Disposal of Radioactive Wastes on Land' in 1957, geological disposal has been suggested as the preferred technique for the long-term disposal of radioactive waste [31]. The recently evolved idea of 'partitioning and transmutation' (P&T) has the potential to lower the risks associated with spent fuel geological disposal. In this method long-lived radionuclides present in spent fuel are chemically partitioned and then converted to shorter-lived, less harmful nuclides via neutron

bombardment. Liquid-liquid extraction can be used to partition specific long-lived elements from spent fuel before they are transmuted. P&T strategy appears to be the best choice for the long-term management of spent fuel due to reducing radiotoxicity, volume, and time required for storage in a repository [32].

1.5 Computational Analysis

Computational analysis is a technique which applies the use of algorithms, programming, and computer hardware to solve scientific problems by creating computational models of a physical phenomenon and then simulating those models using advanced computing techniques. This rapidly growing multi- and interdisciplinary field is becoming indispensable, and it is now universally recognized as the third pillar of science, along with theory and experiment [33].

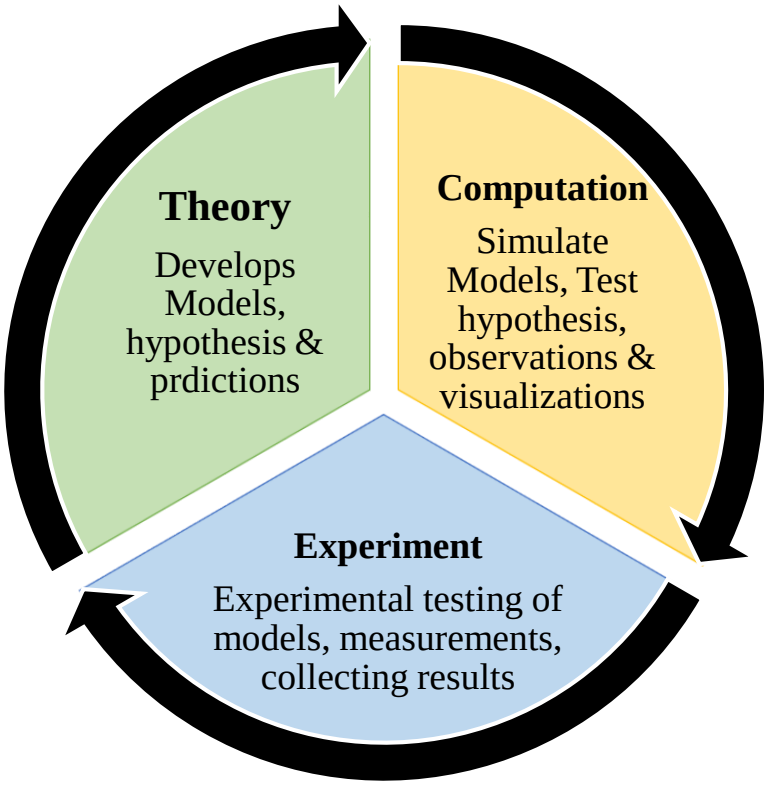

Figure 1.1: Interplay between Three pillars of science

Different computational analytical techniques are being employed in almost every scientific and technical discipline in one way or another, with computational chemistry being one of them. Computational chemistry solves complex chemical problems by calculating the structures, properties, and interactions of atoms and molecules using computer simulations. The most important and widely used computational chemistry methods are molecular mechanics, molecular dynamics, semiempirical, ab-initio and density functional theory (DFT) methods [34]. These computational methods are typically based on two fundamental approaches: classical mechanics and quantum mechanics.

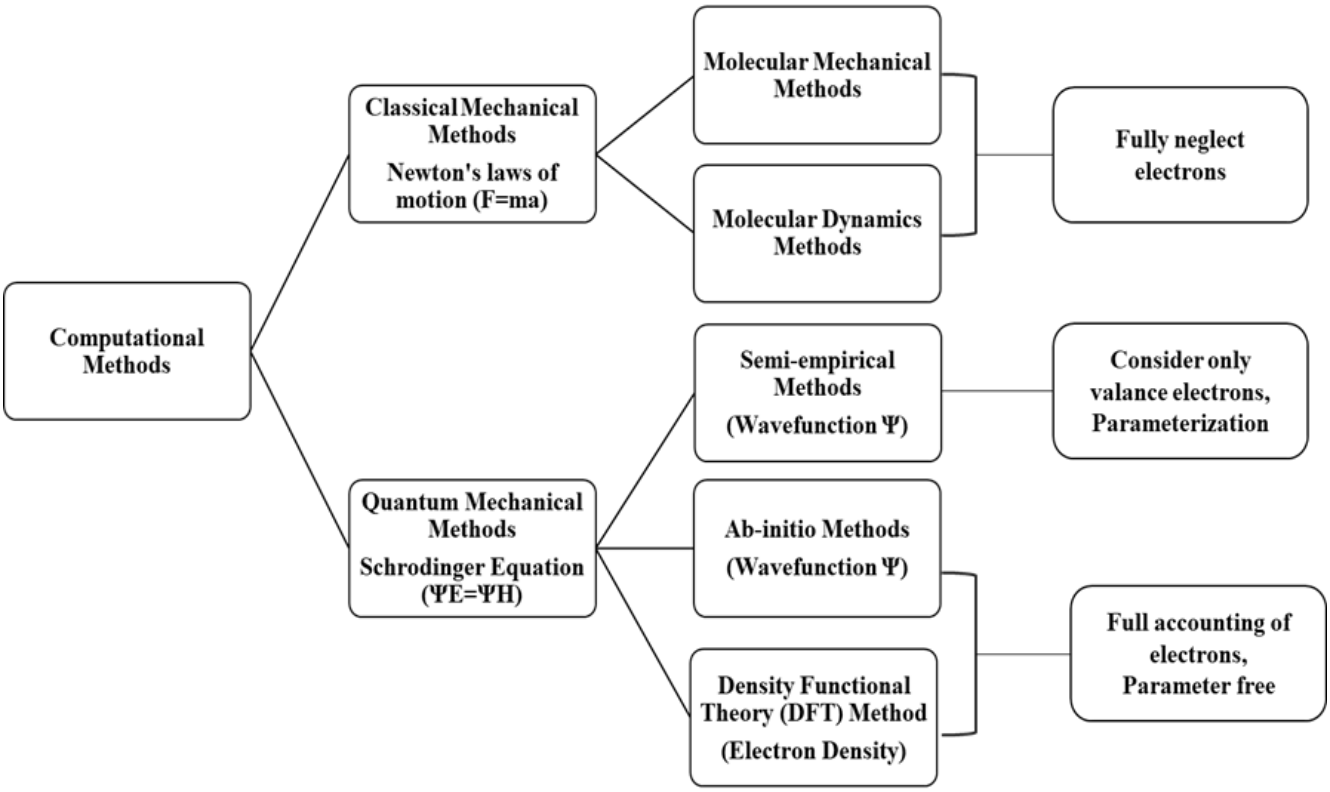

Figure 1.3 Methods of computational chemistry

1.5.1 Classical Mechanical Methods

The classical mechanics-based methods typically include molecular mechanical method and molecular dynamics method, which employ Newton's law [35].

1.5.1.1 Molecular Mechanical Method

Molecular mechanical (MM) method use mathematical expression Born Oppenheimer Approximation which is based on classical mechanics to accurately predict structures, energies, and other properties of molecular systems. As this mathematical expression is a set of potential functions with adjustable parameters, MM methods are commonly referred to as force field methods. In general, the total energy expression for MM force field is:

$$E_{Total} = \sum E_{strech} + \sum E_{bend} + \sum E_{torsion} + \sum E_{VDW} \quad (1.1)$$

In this method a hypothetical mechanical model of a molecule is considered as a collection of balls (atoms) held together by springs (bonds), as depicted in Figure 1.5 [36].

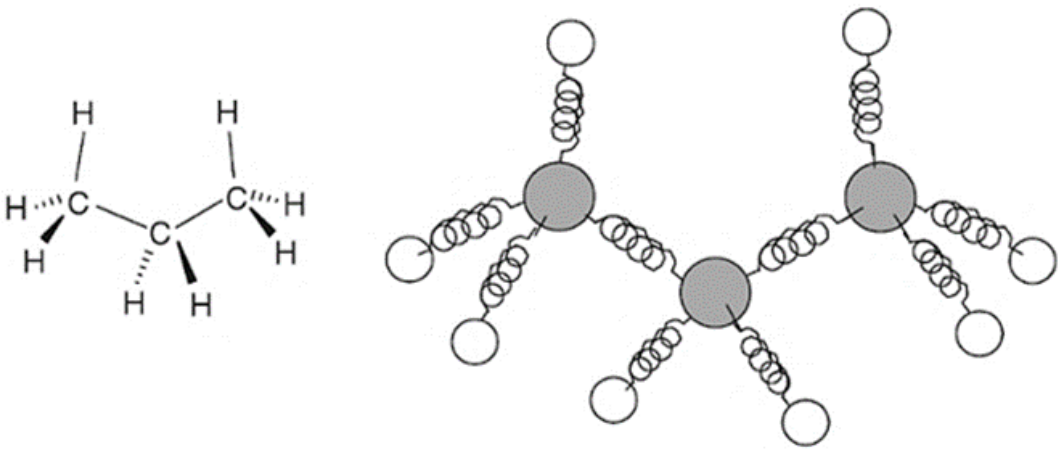

Figure 1.2: Ball-and-spring model of molecule considered in Molecular Mechanical Approach [36]

Though MM methods are simpler, faster, and efficient to determine geometries and energy for small to large molecular systems, such as biomolecules, they are unable to interpret electronic properties because they fully ignore electrons [37].

1.5.1.2 Molecular Dynamics Method

Molecular dynamics (MD) simulations employ Newton's second law of motion (F=ma) to analyze the dynamic conformational changes of atoms in a molecular system as a function of time. MD has the potential to accurately examine the dynamic and thermodynamic characteristics of a

single atom to a large group of atoms, especially in the case of biomolecular systems comprising several thousands of atoms operating across nanoseconds [38], [39].

1.5.2 Quantum Mechanical Methods

In contrast to classical mechanical methods, electrons in quantum mechanical (QM) methods are considered to move under the influence of the nuclei in the molecule. QM methods essentially involve solving the Schrodinger equation within certain approximations to determine the electronic structure, energies and forces acting on the atoms in a molecular system [40], [41]. Besides this these methods provide not only details about potential reaction pathways but also thermodynamic data such as heat of formation. Ab initio methods, semi-empirical methods, and the density functional theory (DFT) are the computational approaches that are based on quantum mechanics [42].

1.5.2.1 Ab-initio Method

Ab initio calculations are widely used to determine the structure, energies and properties of molecular systems including tens to hundreds of atoms and their corresponding electrons. These methods focus on calculating wave functions by solving Schrödinger's equation with various approximations in order to describe atomic orbitals for the determination of molecular properties. The Latin term ab-initio, which means "from the start," suggests that this method does not rely on empirical data about a molecular system. To achieve the best result, these methods employ a convergent strategy that yields precise, excellent results. However, because of the high operational costs and time prerequisites these methods are only effective for small molecules [36], [42].

1.5.2.2 Semi-empirical Method

Compared to the ab initio method, the semi-empirical (SE) method is based on the same formalism, which has significantly reduced the complexity of the calculation without significantly affecting the accuracy by employing additional approximations, such as considering only valance

electrons for calculation, requiring a minimum number of basis sets, and using some empirical parameters. When dealing with bigger systems, the SE methods are preferable to the ab-initio approaches [42], [43].

1.5.2.3 Density Functional Theory Method

Density Functional theory (DFT) method also solves Schrodinger's Equation, but in contrast to the ab initio and SE methods, it derives the electron density function of a molecular system rather than computing a wavefunction. It is typically based on the theorem given by Hohenberg and Kohn in 1964 [42], which says that the ground state energy and properties of a system are distinctively assessed by its electron density, no matter which orbitals (s, p, d, etc.) contribute to it. The calculation of the electron density is independent of the number of electrons, unlike the wavefunction, which becomes substantially more complex with the increase in number of electrons. This electron density is symbolized as $\rho(x, y, z)$, which is the probability of finding an electron per unit volume with the position of electron in x, y, and z coordinates [40], [42]. Over the past couple of decades, density functional theory (DFT) has made considerable strides, and today it offers a wide range of applications in the fields of chemistry and material science to help in studying the behavior of complex molecular systems by performing following operations [44]:

a) Geometry optimization (GO)
b) Single-point energy (SPE) calculation
c) Frequency Calculations
d) Spectroscopic analysis (IR/Raman/ EPR/NMR/UV-visible Spectra)
e) Detailed descriptions of molecular orbitals (bonding properties i.e., ionization energies and electron affinities)

f) Calculation of atomic charges, dipole moments, multipole moments, electrostatic potentials, polarizabilities, etc.

g) Evaluation of solvent effects

h) Noncovalent interactions in extended molecular systems

DFT methods are relatively considered “better” than ab initio methods and are said to be more accurate with lower computational cost.

2 Literature Review

A drawback of energy production using nuclear power plants is the generation of nuclear waste which contains the major portion of fission products and transuranium (TRU) actinide fractions that retain radiotoxicity for hundreds of thousands of years. Because of their strong radioactivity, high toxicity, and large heat release rate, which is obviously a matter of great environmental concern, such elements urgently need to be remediated. The safe and cost-effective long-term disposal of spent nuclear waste has been the subject of extensive research over the past few decades [17], [45]. Among the options considered are geological disposal, sub-seabed disposal, deep borehole disposal, ice-sheet disposal, rock-melt disposal, space disposal, reprocessing, partitioning, and transmutation [46]–[49].

2.1 Partitioning and Transmutation (P&T)

Numerous well-documented studies [32], [50], [51] both at national and international level suggested that, amongst the different strategies, partitioning and transmutation (P&T) strategy is considered as the best possible way to reduce the burden of radiotoxicity and radiogenic heat load associated with spent nuclear waste leading to optimal use of geological repositories. Recently the successful application of P&T scheme and its beneficial effects on a specific repository (Yucca Mountain), from the point of view of its design and operation, accounting for both thermal constraints and peak dose rate constraints has been pointed out [32].

For partitioning of highly radiotoxic components of nuclear waste, multiple separation and purification techniques for example chromatographic separation [52], ion exchange resins separation [53] and supported liquid membrane extraction[54] have been proposed. However, in the last fifty years, the most common wet method, 'liquid-liquid extraction, commonly known as 'solvent extraction,' has been proven to be the most viable separation option for the industrial scale partitioning and transmutation of spent fuel components [55]–[57].

Pu and minor actinides (MA) neptunium, americium, and curium are mainly responsible for the longer life and high radio toxicity of spent nuclear fuel [32], [58], therefore separating these elements would reduce the radiotoxicity, heat load, volume, and lifespan of the remainder waste for long-term storage [32], [59]. PUREX (Plutonium Uranium Redox EXtraction), a solvent extraction process introduced in the 1940s, was among the oldest known reprocessing [60], in which organophosphorus compounds, such as Tri n-butyl phosphate (TBP) (Figure 2.1) [56] diluted in various types of aliphatic hydrocarbon mixtures or in pure dodecane were used as an extractant to recover U and Pu from remainder of the spent fuel [60], [61]. After separation, U(VI) and Pu(IV) are combined to generate a mixed oxide (MOX) substance that can be used as fresh fuel in the recent generation III reactors and fast reactors (FRs) [62] because of which P&T scheme is expected to extend the nuclear fuel resources on earth about 100 times [50].

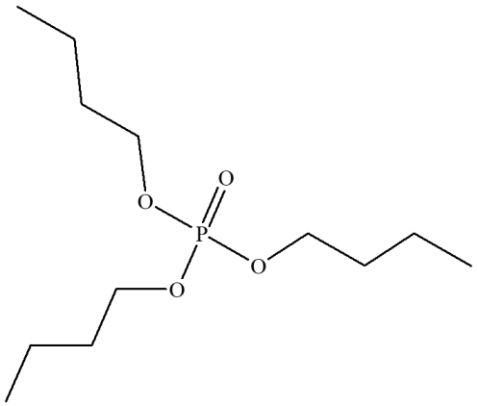

Figure 2.1 Chemical Structure of tri n-butyl phosphate extractant

Studies Showed that TBP allows a selective and nearly quantitative recovery of tetra- and hexavalent actinides [typically U(VI) and Pu(IV)] with high decontamination factors in a range of 10^6-10^8 [45], [63], consequently decreasing the volume about 80%, radiotoxicity about 90% and the decay heat of the PUREX raffinate (remaining waste) [59], [64]. In order to achieve further significant reduction in the radiotoxicity (up to the reduction factors higher than 100) [65] and decay time (to achieve natural U levels in 300 years rather than 9000 years) [23] of the remaining waste, there is a need to recover and transmute also MAs.

2.2 Minor actinides (MA) separation from PUREX raffinate

PUREX technique has been extended for the extraction of neptunium (Np) along with U and Pu (advanced PUREX) [66], [67], but unfortunately americium and curium cannot be separated directly in this process [68], requiring additional processes for their separation. However, these trivalent minor actinides are not industrially separated.

Several extraction processes which make use of different extractants have been developed initially concerned with the co-extraction of minor actinides (MA) along with the lanthanides (Ln) from the PUREX raffinate [51], [69], with subsequent second step extraction to separate these actinides from the Ln [55]. Among the processes related to this idea, the most important for An(III) and Ln(III) co-extraction are TRUEX (USA) uses ‘octyl(phenyl)-N,N-diisobutyl Carbamoyl Methyl Phosphine Oxide’ (CMPO) as the extractant [70], DIAMEX (France) uses malonamides as the extractant [71], and TRPO (China) uses a mixture of tri-alkyl phosphine oxides as the extractant [50] while for An(III)/Ln(III) separation are TALSPEAK (USA) based on the use of acidic organophosphorus extractants [59] and SANEX (Europe) which uses different S and N bearing extractants [72], [73].

2.2.1 An(III)/Ln(III) separation is a challenging task

To transmute the trivalent actinides Am(III) and Cm(III) causing long-lasting radiotoxicity into less harmful shorter-lived elements, it is vitally important to separate them from the trivalent lanthanides Ln(III) present in the raffinate. The major reason is high neutron-capture cross-sections of the lanthanides thus acting as neutron poisons, hinders an efficient transmutation of the trivalent minor actinides, and therefore, the two groups of elements have to be separated [74]. But this An(III)/Ln(III) separation is the most demanding and difficult task in spent nuclear fuel reprocessing, due to their similar physiochemical properties (identical oxidation state and ionic radii) combined with the unfavorable mass ratio (An/Ln is ca. 1:40) [23], [75]. The only distinguishing factor is how their respective valance f-orbitals are distributed in space. Space distribution of actinide 5f orbitals is larger than that of lanthanide 4f orbitals. As the lanthanide 4f orbitals are localized within the atomic core, they contribute very little to metal-ligand bonding. As a consequence, the actinides form stronger covalent bonds with the soft donor ligands [53]. Taking advantage of this attribute of increased covalency of trivalent actinides many studies concerning the separation of lanthanides(III) from actinide(III) have been carried out and reviewed in detail [57], [68], [76].

Thus, It has been suggested that this An(III)/Ln(III) separation can be achieved by using soft donor ligands (containing S and N atoms) as they have a certain selectivity for An(III) over Ln(III) [77]–[79]. Among Them, a commercial reagent named Cyanex-301 [80], which is an acidic S-bearing extractant belonging to the family of organo-dithio-phosphinates, bis(2,4,4-trimethylpentyl) dithiophosphinic acid (HBTMPDTP), has already been tested on genuine solutions and showed a high efficiency for An(III)/Ln(III) separation. For example, In 1996, Zhu [81] found that this Cyanex-301 reagent has excellent selectivity for Am(III) over Eu(III), with

the separation factor up to 5000. However, Cyanex-301 reagent's biggest downfall is that it is extremely sensitive to feed acidity i.e., fails to be extracted at lower pH (pH < 3) [82] and generates a sulphur-bearing waste that can be difficult to manage [83]. Furthermore, as reported in 1996, [84] Cyanex-301 is radiolytically unstable, and its extraction selectivity toward Am over lanthanides reduces after being exposed to radiations.

In the course of subsequent research, scientists came up with the compound known as 6,6'-bis(5,5,8,8-tetramethyl-5,6,7,8-tetrahydro-1,2,4-benzotriazin-3-yl)-2,2-bipyridine (CyMe4-BTBP) (Fig.) [85], which is a soft, heterocyclic N-donor ligand. To date, this molecule has been regarded as the most promising ligand for usage in a SANEX (Selective Actinide Extraction) process due to its high selectivity for An(III) over Ln(III) and enhanced radio- and hydrolytic stability [86]. In 2008 [87], at the Institute for Transuranium Elements in Karlsruhe, 99.9% of the actinides in the feed solution were removed with extremely high decontamination factors for Am (7,000) and Cm (1,000).

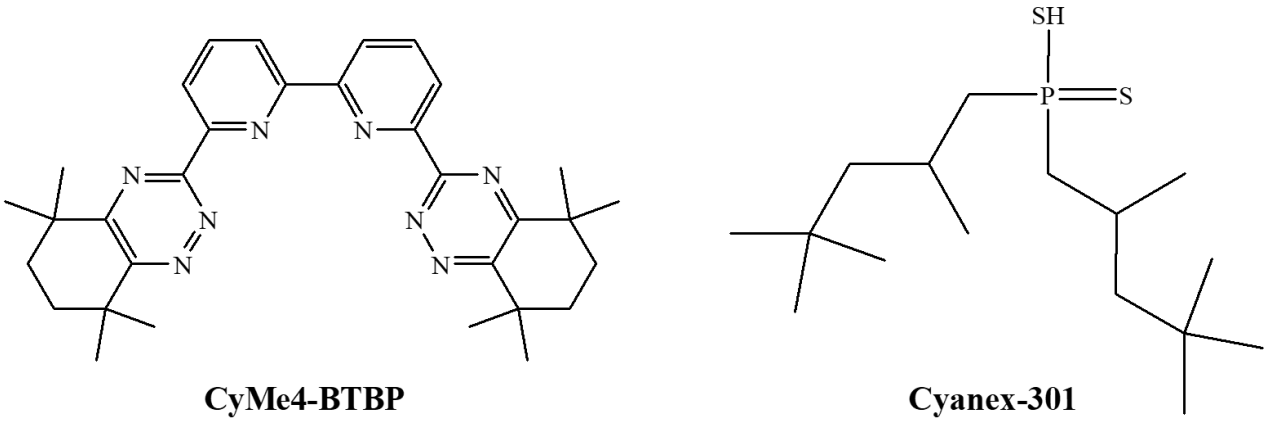

CyMe4-BTBP **Cyanex-301**

Figure 2.2 Chemical structure of a) CyMe4-BTBP, and b) Cyanex-301 reagent

However, CyMe4-BTBP does still have some drawbacks [88]. It is negatively impeded by excessive ligand-cation complexation and extremely slow extraction kinetics. The first issue would require more extraction stages (i.e., a bigger space, more volume, more expense), but the second issue would make it difficult to recover cations back prior to the conversion and fuel manufacture

processes [89]. Thus, the design and assessment of new N and S donor ligands which show improved kinetics, radiolytic stability and back-extraction properties is on-going.

2.3 Problem Statement

Nuclear power, with its benefit of relatively low waste production, is set to overtake fossil fuels as the primary means of generating electricity in the following years. However, spent nuclear waste is harmful because it contains various radioactive nuclides with long half-lives, such as uranium, plutonium, fission products, and minor actinides. While uranium, plutonium, and a number of other fission products can be easily recovered using various extractants to lessen the radiotoxicity of spent nuclear waste, but minor actinides, particularly Am^{+3}, are difficult to extract. Actually, the presence of trivalent Eu^{+3} in the waste hinders the extraction of trivalent Am^{+3} due to their identical oxidation states, ionic radii, and physiochemical properties. This separation of Am^{+3} from Eu^{+3} is therefore a really challenging problem requiring an extractant that is more selective towards Am^{+3} than Eu^{+3}. This research will contribute to the computational design of such extractants and to computationally evaluate the extraction behavior of Am and Eu.

2.4 Proposed Solution

As soft ligands are capable of coordinating with both Am and Eu. Therefore, in this research, organo phosphinodithioic acid ligand and its derivatives were modelled and studied using computational methods. Following that, these ligands were then employed to study the extraction behavior of Am from Eu.

3 Methodology

The primary focus of this study was to perform DFT calculations to analyze the extraction behavior of trivalent Americium and Europium by using derivatives of phosphinodithioic acid as ligands. Three major steps comprise the methodology are presented below:

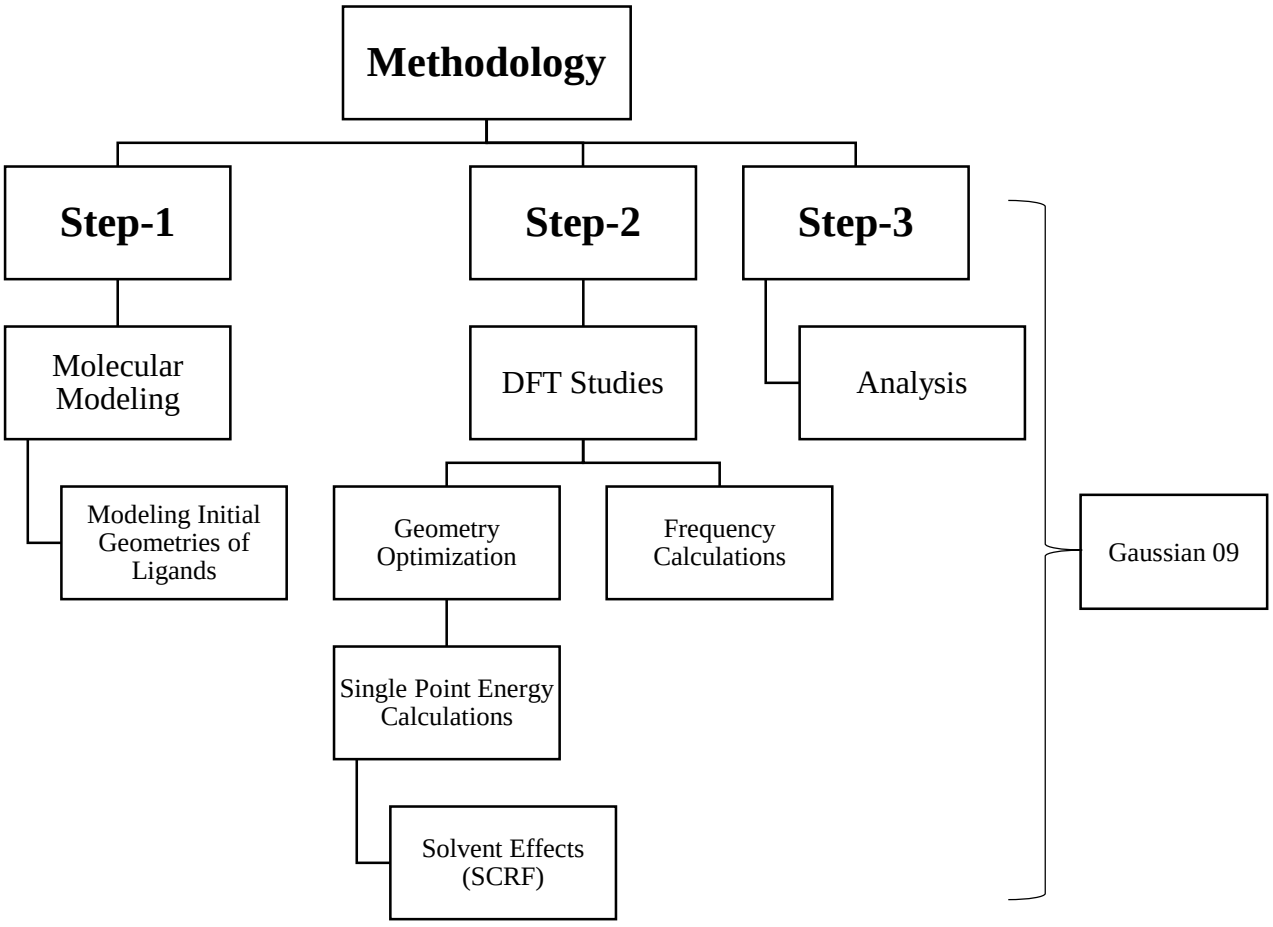

3.1 Molecular Modeling

All initial geometries of ligands and their complexes with europium and americium nitrates were modeled by using GUI Gauss-View06. These modeled geometries were then optimized using Gaussian 09 software in Linux environment on SINES Supercomputer and output geometries were visualized by using Molden software.

3.1.1 Gauss View06

GaussView06 is a graphical user interface commonly used with Gaussian to make it easy to set up various Gaussian calculations. It helps to draw 3D chemical models of molecular systems by using its advanced molecule builder, to generate and run Gaussian input files without any need for using command line instructions and to graphically (e.g., plots, spectra, animated vibrations etc.) interpret the results of Gaussian output files by using its excellent visualization features [90].

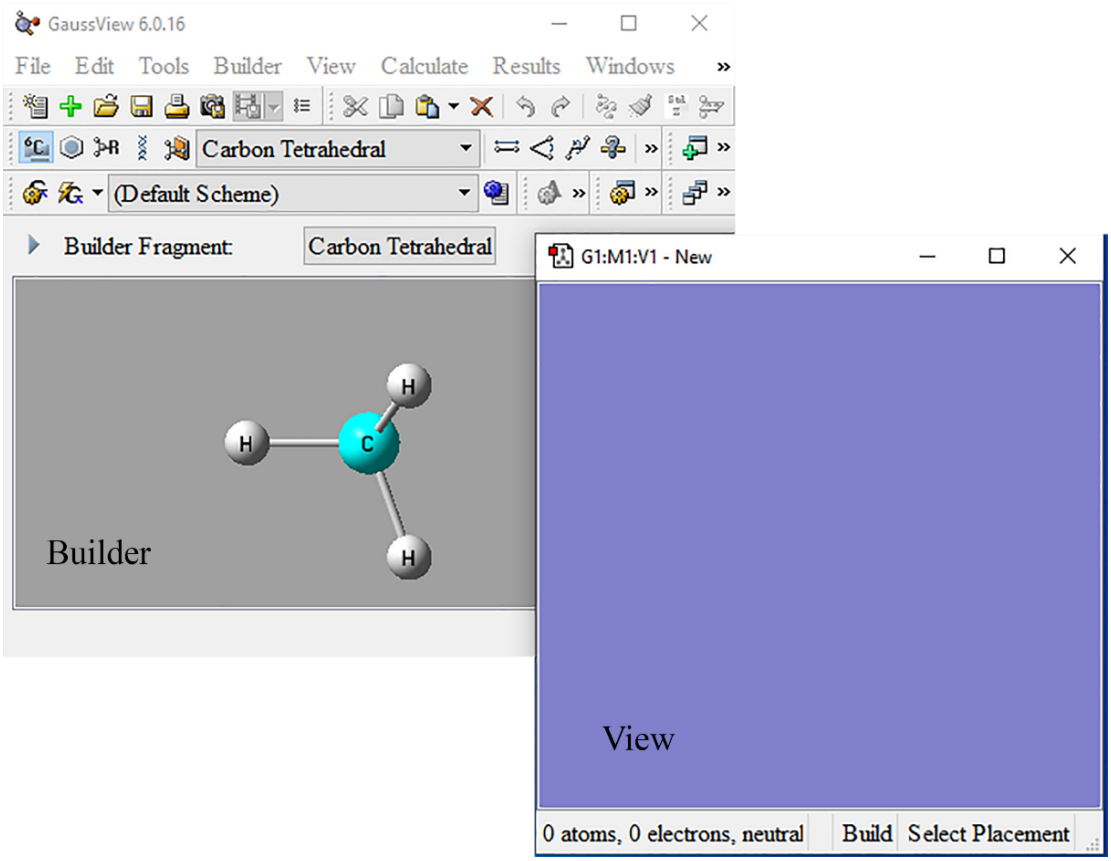

Figure 3.1 Gaussview06 builder and view interface

3.1.2 Gaussian-09

Gaussian is a general purpose software package (http://www.gaussian.com/), first developed by John Pople and his research associates in 1970 as Gaussian-70 [91], and now extensively used as its newest version Gaussian-09 [42]. Chemists, chemical engineers, biochemists, and other material scientists use this software—which is actually a suite of programs with MM, ab initio, semiempirical, and DFT methods—to carry out various chemical and biochemical operations computationally. Gaussian has a number of built-in standard basis sets, such as STO-3G, 3-21G, 6-21G, 4-31G, 6-31G, LANL2DZ, SDD, and others, which the user can access quickly and efficiently [42]. A basis set is simply a set of functions coupled linearly to mathematically describe the molecular orbitals of a system in order to perform quantum chemical calculations [43].

3.2 DFT Studies

In DFT calculations, the electron density of a system is used to learn more about the electronic structure (ground state), energies, and characteristics of a molecule. This approach provides a broader range of density functionals such as BLYP, B3LYP, BPLYP, BP86, PBE0, CAM-B3LYP, and others [42], [44], each with its own set of features and applications. Using the DFT approach, the following operations were performed in this study:

a) Geometry optimization of ligands and their complexes with Am and Eu metals

b) Frequency Calculations

c) Single point energy (SPE) calculations

d) Solvent effect/SCRF calculations

3.2.1 Geometry Optimization

Geometry optimization is a process of finding the optimal spatial arrangement of atoms in a molecule by means of overall energy minimization of the system [92]. Geometry optimization

of all the ligands and their complexes with Am and Eu was performed with DFT method using B3LYP hybrid functional and the basis set e.g., SDD, (Stuttgart-Dresden effective core potential).

3.2.1.1 B3LYP Functional

B3LYP (Becke's three-parameter exchange with Lee, Yang, and Parr correlation functional) [44] is the most popular and extensively used hybrid functional in quantum chemistry because of its remarkable potential to precisely predict molecular structures and other properties [92].

3.2.1.2 SDD Basis set

The SDD is a Gaussian incorporated basis set that unites DZ and the Stuttgart-Dresden effective core potential (ECP) basis sets to lower the computational cost caused by the high number of electrons in metals, particularly heavy metals [44] and transition metal [93].

3.2.2 Frequency calculation

All of the optimized geometries were validated by frequency calculations, which involved determining the modes of nuclear vibrational motion in a molecular system using the same basis set as was employed in the geometry optimization process. None of the frequency calculations generated imaginary frequencies showed that the optimized geometries are true energy minima.

3.2.3 Single point energy calculations

To determine the electronic energy of a certain arrangement of atoms, Single Point Energies (SPE) in the gas phase and Self-Consistent Reaction Field (SCRF) calculations using n-dodecane as a solvent were carried out on all the optimized geometries. SPE calculations were run using DFT/B3LYP/SDD level in the gas phase and solvent phase for all optimized geometries.

3.2.4 Molden

Molden is a very useful free visualization tool developed for pre and post evaluation of quantum chemical simulations results. It is not only limited to graphically visualize the results of

output files produced by other programs but can also perform several other operations such as calculation of electrostatic potentials (ESP), orbital/molecular density, and distributed multipole analysis (DMA).

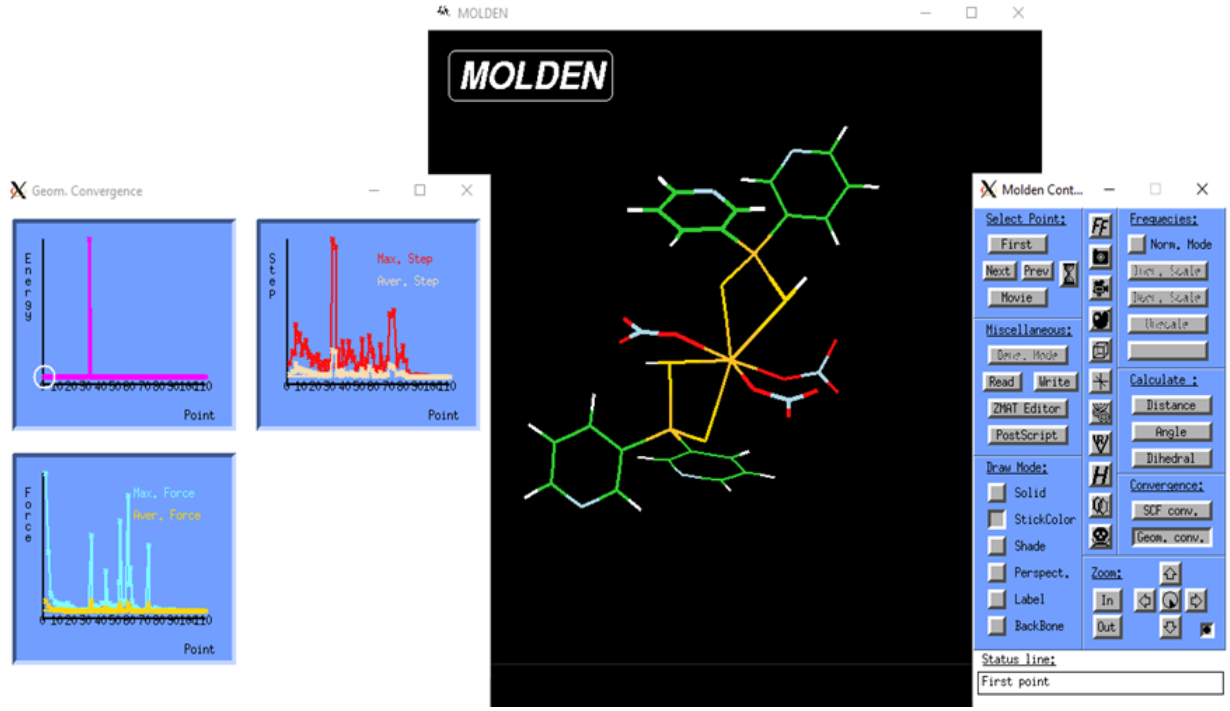

Figure 3.2 Molden: a graphical visualization tool

Molden supports output files from many computational chemistry packages such as gaussian, MOPAC etc. [94]. In this work, molden was used on a Linux-based supercomputer to read gaussian output files and graphically interpret several key parameters such as total energies, step size, forces, animation of reaction routes, and normal modes of vibration.

4 Results and Discussion

Nuclear reactors produce hazardous nuclear waste, which contains several radioactive nuclides with long half-lives, including major actinides (U & Pu), fission products, and minor actinides. The extraction of these radioactive nuclides, in particular minor actinides, is necessary for the safe and long-term disposal of this waste. However, because of actinides and lanthanides similar physiochemical properties, minor actinides, especially Am^{+3}, are difficult to separate from trivalent lanthanides, i.e., Eu^{+3}. In this research, organo phosphinodithioic acid ligand, its four derivatives and their complexes with americium and europium were modeled and analyzed computationally to study the extraction behavior of these elements.

4.1 Molecular Modeling

4.1.1 Organo phosphinodithioic acid ligands

To study the extraction behavior of Eu and Am, organo phosphinodithioic acid ligand and its four derivatives were first modeled in gaussview and then optimized using Gaussian 09 at the energy level of B3LYP/SDD hybrid density functional methods. Table 4.1 lists the abbreviations and nomenclature of these modeled ligands.

Table 4.1 Derivatives of organo phosphinoodiothioic acid ligands

Sr.No	Abbreviations	Ligand Names
01	$BphPT_2$	benzyl(phenyl) phosphinodithioic acid
02	$P2P2PT_2$	pyridine-2-yl(pyridine-2-ylmethyl) phosphenodithioic acid
03	$P3P3PT_2$	pyridine-3-yl(pyridine-3-ylmethyl) phosphenodithioic acid
04	$P2P3PT_2$	pyridine-2-ylmethyl(pyridine-3-yl) phosphinodithioic acid
05	$PPPT_2$	pyridazin-3-yl(pyridazin-3-ylmethyl) phosphinodithioic acid

All these ligands differ from each other on the basis of different electron withdrawing ability due to nitrogen atom in the ring. Figure 4.1 shows the general structure of organo phosphenodithioic acid ligands. Figure 4.2 depicts the Optimized three-dimensional geometries of organo phosphenodithioic acid ligand and its four derivatives.

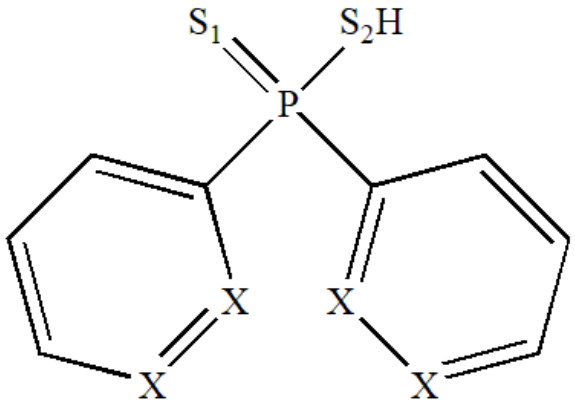

Figure 4.1 General structure of organo phosphinodithioic acid ligands

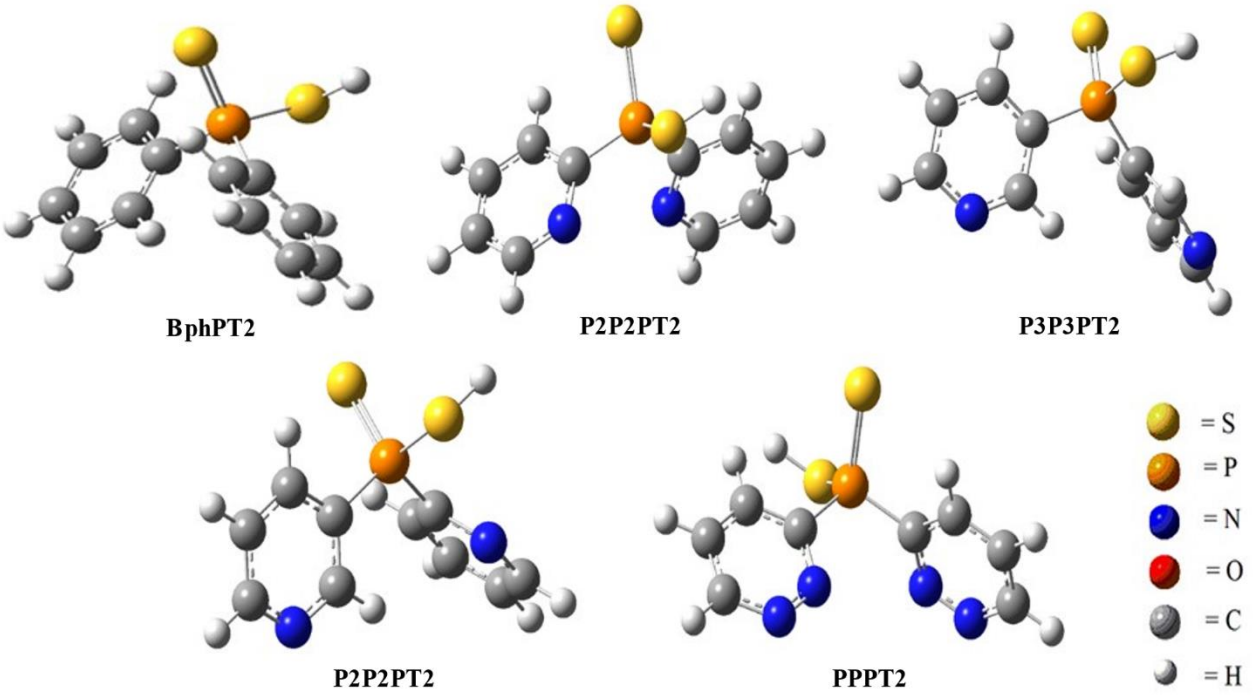

Figure 4.2 Optimized 3-D geometries of five derivatives of organo phosphenodithioic acid ligands

These optimized ligands were then used to model metal ligand (M-L) complexes of Am and Eu metals with the ratio of 1:1, 1:2 and 1:3. In all these complexes, central metal atom is bonded to one, two or three organo phosphinodithioic acid ligands respectively. Figure 4.3 a, b and c shows general structures of 1:1, 1:2 and 1:3 M-L complexes.

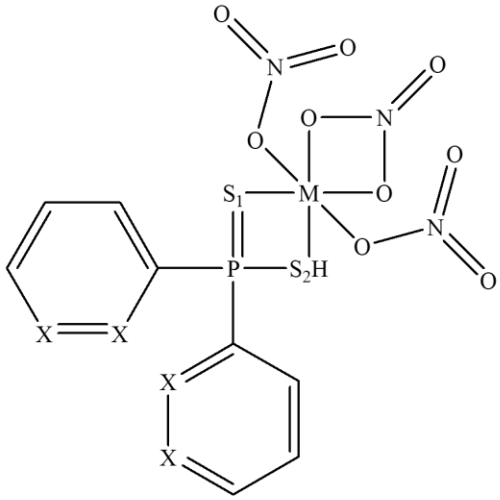

(a) 1:1 M-L complex

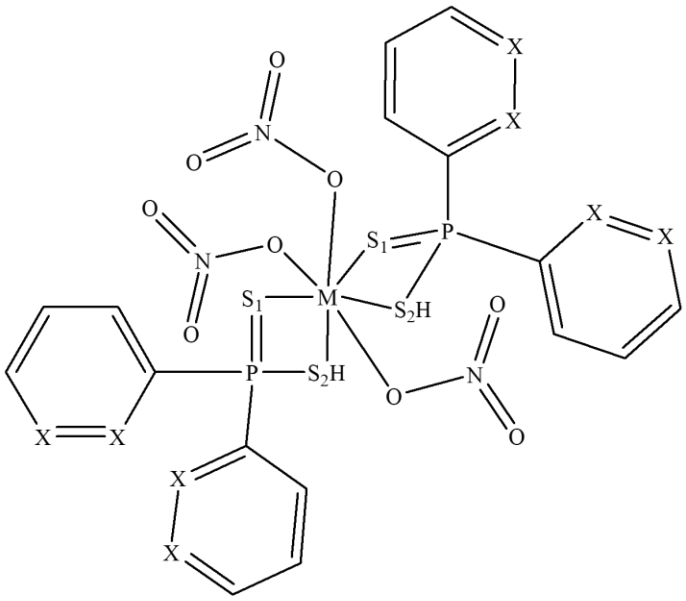

(b) 1:2 M-L complex

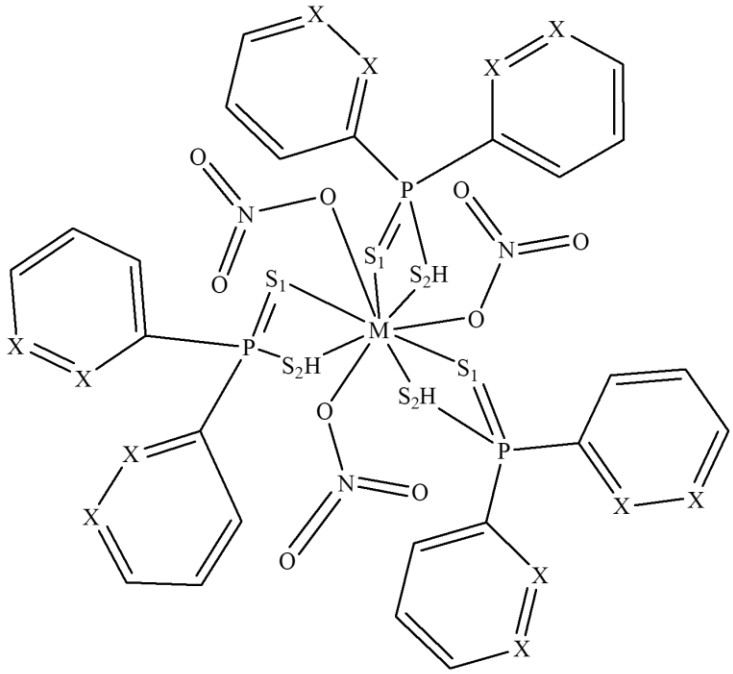

(b) 1:3 M-L complex

X= C or N & M= Am or Eu

Figure 4.3 General structure of 1:1, 1:2 and 1:3 metal-ligand complexes

4.2 Geometry optimization

The modeled geometries of 1:1, 1:2 and 1:3 M-L complexes of Am and Eu were optimized using B3LYP (Becke's three-parameter exchange with Lee, Yang, and Parr correlation) functional in combination with higher basis set like SDD. The relative energies of Am and Eu complexes with organophosphino dithioic acid ligand and its derivatives are presented in table 4.2. The eq. 4.1 shows the reaction followed in this study.

$$M(NO_3)_3 + nL \rightarrow MLn\text{-}(NO_3)_3 \quad \text{Eq. 4.1}$$

The total binding energy/relative energy was calculated using the equation below:

$$\Delta E = (\text{Total energy of Products}) - (\text{Total energy of Reactants}) \quad \text{Eq. 4.2}$$

$$\text{e.g., } \Delta E = 627.51^{*}[\ (E_{MLn\text{-}(NO3)3\ Complex}) - (E_{M(NO3)3} + E_{nL})] \quad \text{Eq. 4.3}$$

Table 4.2 Relative energies of 1:1, 1:2 and 1:3 Am/Eu complexes in gas phase and n-dodecane solvent

Ligands	Eu(NO3)3:L			Am(NO3)3:L			Energy level
	1:1	1:2	1:3	1:1	1:2	1:3	
Ligand-01 BphPT2	-12.42 73.44	-448.71 -18.07	--*	-7.96 169.17	-15.96 -55.38	-539.38 -13.98	Gas phase n-dodecane
Ligand-02 P2P2PT2	-19.09 -4.24	-467.32 43.20	--*	-12.78 -0.03	-57.67 32.16	--*	Gas phase n-dodecane
Ligand-03 P3P3PT2	-746.59 -740.16	-457.29 -39.34	--*	-15.62 -5.92	-18.67 -34.27	--*	Gas phase n-dodecane
Ligand-04 P2P3PT2	--*	-475.30 -51.96	--*	-31.79 -20.70	-43.07 -12.82	--*	Gas phase n-dodecane
Ligand-05 PPPT2	-8.21 5.45	-43.19 -53.87	--*	-19.77 -12.74	-16.29 -50.61	--*	Gas phase n-dodecane

*= No lower point found to calculate minima.

4.2.1 Am/Eu-BphPT2 Ligand Complexes

Computational results revealed that the formation of 1:1 Am-BphPT2 complex (Figure 4.4a) is an exothermic reaction with -7.96 Kcal/mol energy in the gas phase (highly endothermic

with energy 169.17 Kcal/mol in n-dodecane solvent) relative to separate metal salt and ligand (Table 4.2). Similarly, the formation of 1:1 Eu-BphPT2 complex (Figure 4.4 b) is an exothermic reaction with energy -12.42 Kcal/mol (endothermic, 73.44 Kcal/mol) relative to the separate metal salt and ligand. Am and Eu are the f-block elements that can form complexes with up to nine coordination numbers. Therefore, to optimize the metal: ligand ratio complexes (1:2 & 1:3) of Eu and Am salts with ligand were designed and optimized. The relative energies computed for 1:2 Am-BphPT2 complex (Figure 4.4 c) are -15.96 Kcal/mol (-55.38 Kcal/mol) relative to the separate metal salts and BphPT2 ligand. In contrast for the formation of 1:2 Eu-BphPT2 complex (Figure 4.4 d), the relative energies computed is -448.71 Kcal/mol (-18.07 Kcal/mol). Furthermore, the formation of the 1:3 Am-BphPT2 complex (Figure 4.4 e) is highly exothermic, with energy -539.46 Kcal/mol in the gas phase compared to -13.93 Kcal/mol in the n-dodecane solvent. But 1:3 Eu-BphPT2 complex formation was not succeeded, as no lower energy point was found to calculate the energy minima. The comparison of relative energies of Am/Eu-BphPT2 complexes with increasing metal: ligand ratios is presented below:

Am complexes in gas phase:

Ratio	1:1 Am-BphPT2 → 1:2 Am-BphPT2 → 1:3 Am-BphPT2
ΔE	-8.46 Kcal/mol → -16.04 Kcal/mol → -539.46 Kcal/mol

Am complexes in n-dodecane solvent:

Ratio	1:1 Am-BphPT2 → 1:2 Am-BphPT2 → 1:3 Am-BphPT2
ΔE	169.17 Kcal/mol → -55.38 Kcal/mol → -13.93 Kcal/mol

Eu complexes in gas phase:

Ratio	1:1 Eu-BphPT2 → 1:2 Eu-BphPT2 → 1:3 Eu-BphPT2
ΔE	-12.42 Kcal/mol → -448.71 Kcal/mol → not optimized

Eu complexes in n-dodecane solvent:

Ratio	1:1 Eu-BphPT2 → 1:2 Eu-BphPT2 → 1:3 Eu-BphPT2
ΔE	73.44 Kcal/mol → -18.07 Kcal/mol → not optimized

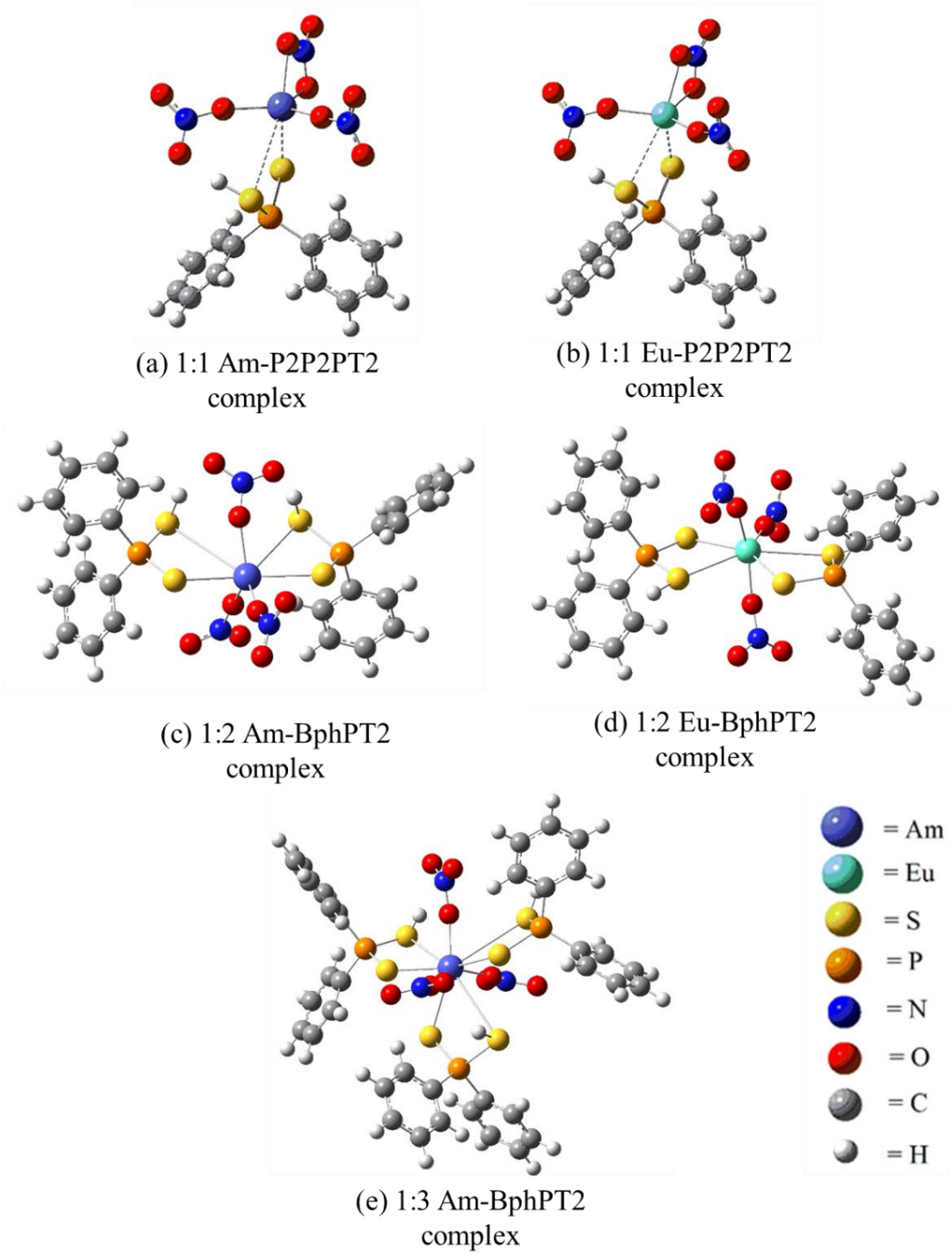

Figure 4.4 Three-dimensional optimized geometries of Am/Eu-BphPT2 complexes

Analyzing the data for Am/Eu-BphPT2 complexes, it was revealed that for a fixed number of nitrate ions but increasing number of BphPT2 ligand in 1:1, 1:2 and 1:3 Am/Eu-BphPT2 complexes, the relative energy for the formation of complexes decreases for 1:2 complexes, however, increases for 1:3 complexes, as the coordination number increases. The relative energy for the formation of Am-BphPT2 complex decreases from 169.17 Kcal/mol to -55.38 Kcal/mol when the metal ligand ratio was changed from 1:1 to 1:2. However, when the ratio wase increased from 1:2 to 1:3 the relative energy for the formation of Am-BphPT2 complex in n-dodecane solvent increased from -55.38 Kcal/mol to -13.98 Kcal/mol. The reason could be the increased steric hindrance introduced by the bulky BphPT2 ligands on the Am metal renders the complex unstable.

4.2.2 Am/Eu P2P2PT2 Ligand complexes

Am-P2P2PT2 complex (Figure 4.5 a) formation is an exothermic reaction, both in gas and solvent, with a -12.78 Kcal/mol energy in the gas phase (-0.03 Kcal/mol in the solvent n-dodecane). Similarly, the formation of 1:1 Eu-P2P2PT2 complex (Figure 4.5 b) is also an exothermic reaction with energy -19.09 Kcal/mol (-4.24 Kcal/mol) relative to the separate metal salt and ligand. The relative energy calculated for 1:2 Am-P2P2PT2 complex (Figure 4.5 c) is -57.67 Kcal/mol (32.16 Kcal/mol) relative to the separate metal salts and P2P2PT2 ligand. In contrast for the formation of 1:2 Eu-P2P2PT2 complex (Figure 4.5 d), the relative energy computed is -467.32 Kcal/mol (43.20 Kcal/mol). However, the formation of 1:3 Am/Eu-P2P2PT2 complexes was unsuccessful because no lower energy point was located to compute the energy minima.

In n-dodecane solvent:

Ratio	1:1 Am-P2P2PT2 → 1:2 Am-P2P2PT2 → 1:3 Am-P2P2PT2
ΔE	-0.03 Kcal/mol → 32.16 Kcal/mol → not optimized

Ratio	1:1 Eu-P2P2PT2 → 1:2 Eu-P2P2PT2 → 1:3 Eu-P2P2PT2
ΔE	-4.24 Kcal/mol → 43.20 Kcal/mol → not optimized

Evaluating the calculated relative energy data for Am/Eu-P2P2PT2 complexes, it was revealed that for a fixed number of nitrate ions but increasing number of P2P2PT2 ligand in 1:1 and 1:2 Am/Eu-P2P2PT2 complexes, the relative energy for the formation of complexes in n-dodecane solvent increases as the coordination number increases. The relative energy for the formation of the Am-P2P2PT2 complex increased from -0.03 Kcal/mol to 32.16 Kcal/mol when the metal ligand ratio was increased from 1:1 to 1:2, and similarly for the formation of the Eu-P2P2PT2 complex, it increased from -4.24 Kcal/mol to 43.20 Kcal/mol.

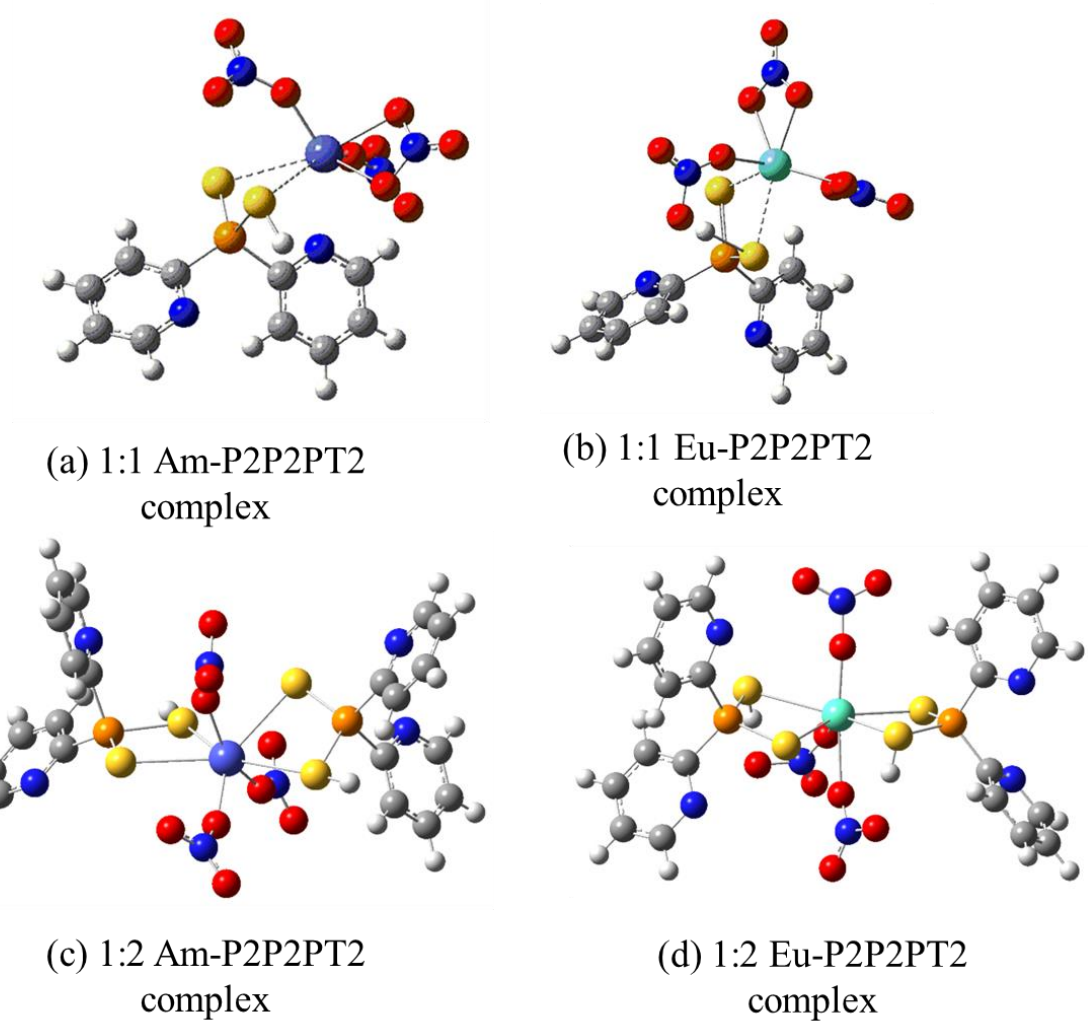

Figure 4.5 Three-dimensional optimized geometries of Am/Eu-P2P2PT2 complexes

4.2.3 Am/Eu P3P3PT2 Ligand complexes

According to obtained computational results (Table 4.2), Am-P3P3PT2 complex (Figure 4.6 a) formation is an exothermic reaction with a -15.62 Kcal/mol energy in the gas phase (-5.92 Kcal/mol in the solvent n-dodecane). Likewise, the formation of 1:1 Eu-P3P3PT2 complex (Figure 4.6 b) is also an exothermic reaction with energy -746.59 Kcal/mol (-740.16 Kcal/mol) relative to the separate metal salt and ligand. The relative energy obtained for 1:2 Am-P3P3PT2 complex (Figure 4.6 c) is -18.67 Kcal/mol (-34.27 Kcal/mol in n-dodecane solvent) relative to the separate metal salts and P3P3PT2 ligand. On the other hand, the relative energy calculated for the formation of the 1:2 Eu-P3P3PT2 complex (Figure 4.6 d) is -457.29 Kcal/mol (-39.34 Kcal/mol). However, the formation of 1:3 Am/Eu-P3P3PT2 complexes was failed as no lower energy point was obtained to compute the energy minima.

In n-dodecane solvent:

Ratio	1:1 Am-P3P3PT2 → 1:2 Am-P3P3PT2 → 1:3 Am-P3P3PT2
ΔE	-5.92 Kcal/mol → -34.27 Kcal/mol → not optimized
Ratio	1:1 Eu-P3P3PT2 → 1:2 Eu-P3P3PT2 → 1:3 Eu-P3P3PT2
ΔE	-740.16 Kcal/mol → 39.34 Kcal/mol → not optimized

Analyzing the data for Am/Eu-P3P3PT2 complexes, it was revealed that for a fixed number of nitrate ions but increasing number of P3P3PT2 ligand in 1:1 and 1:2 Eu-P3P3PT2 complexes, the relative energy for the formation of complexes in n-dodecane solvent increased as the coordination number increased, whereas for the formation of 1:1 and 1:2 Am-P3P3PT2 complexes the relative energy decreased as the coordination number increased. When the metal ligand ratio was increased from 1:1 to 1:2, the relative energy for the formation of the Eu-P3P3PT2 complex increased from -740.16 Kcal/mol to 39.34 Kcal/mol, in contrast for the formation of the Am-P3P3PT2 complex, it decreased from -5.92 Kcal/mol to -34.27 Kcal/mol.

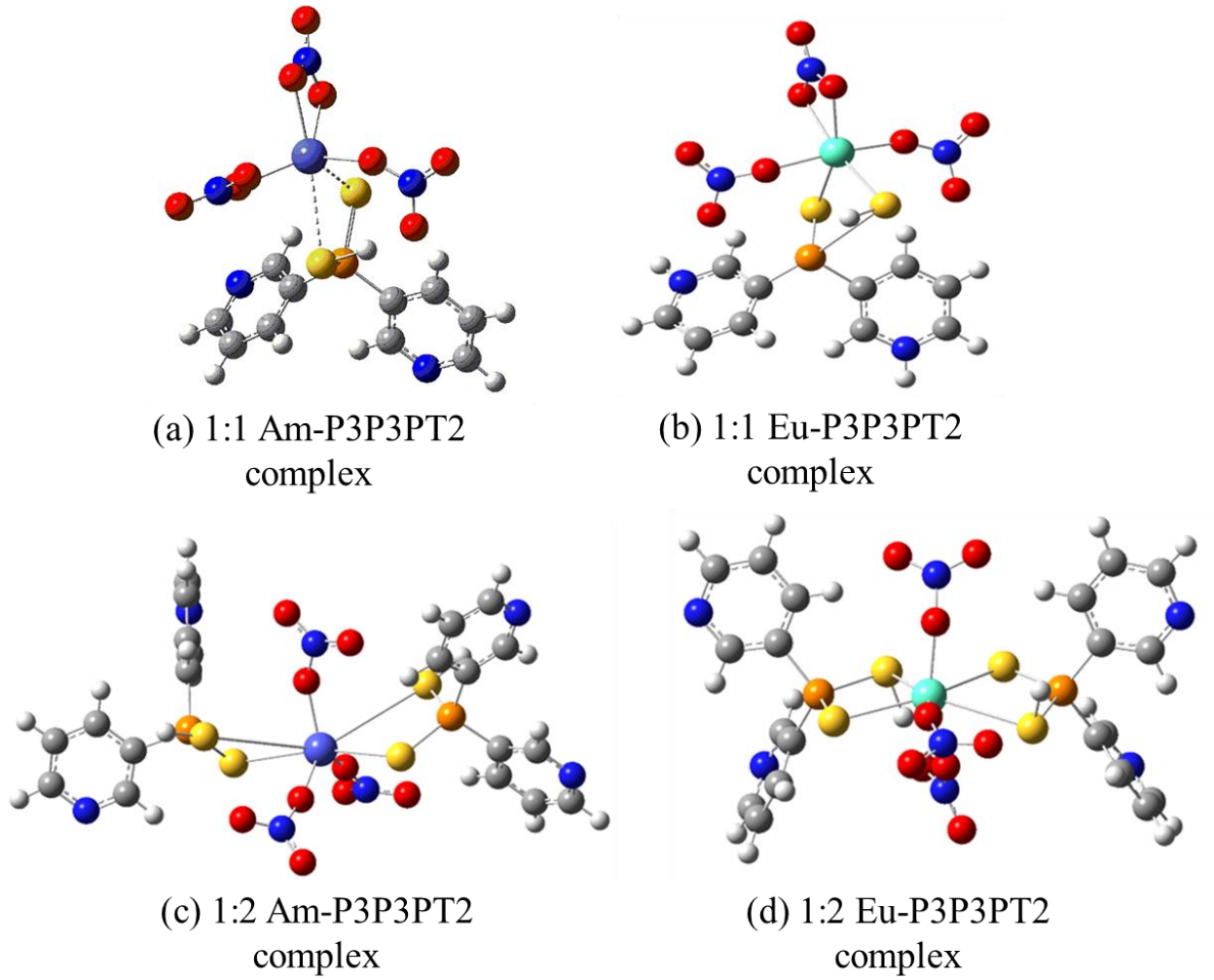

Figure 4.6 Three-dimensional optimized geometries of Am/Eu-P3P3PT2 complexes

4.2.4 Am/Eu P2P3PT2 Ligand complexes

Computational results (Table 4.2) revealed that, Am-P2P3PT2 complex (Figure 4.7 a) formation is an exothermic reaction with a -31.79 Kcal/mol energy in the gas phase (-20.70 Kcal/mol in the solvent n-dodecane). The formation of 1:1 Eu-P2P3PT2 complex (Figure 4.7 b) is also an exothermic reaction with the relative energy of -746.59 Kcal/mol (-740.16 Kcal/mol). In comparison to the individual metal salts and P2P3PT2 ligand, the relative energy calculated for the 1:2 Am-P2P3PT2 complex (Figure 4.5 c) is -43.07 Kcal/mol (-12.82 Kcal/mol). The relative energy required to form the 1:2 Eu-P2P3PT2 complex, on the other hand, is -475.30 Kcal/mol (-

51.96 Kcal/mol) (Figure 4.5 d). However, no lower energy point was found to calculate the energy minima, hence the formation of 1:3 Am/Eu-P2P3PT2 complexes was unsuccessful.

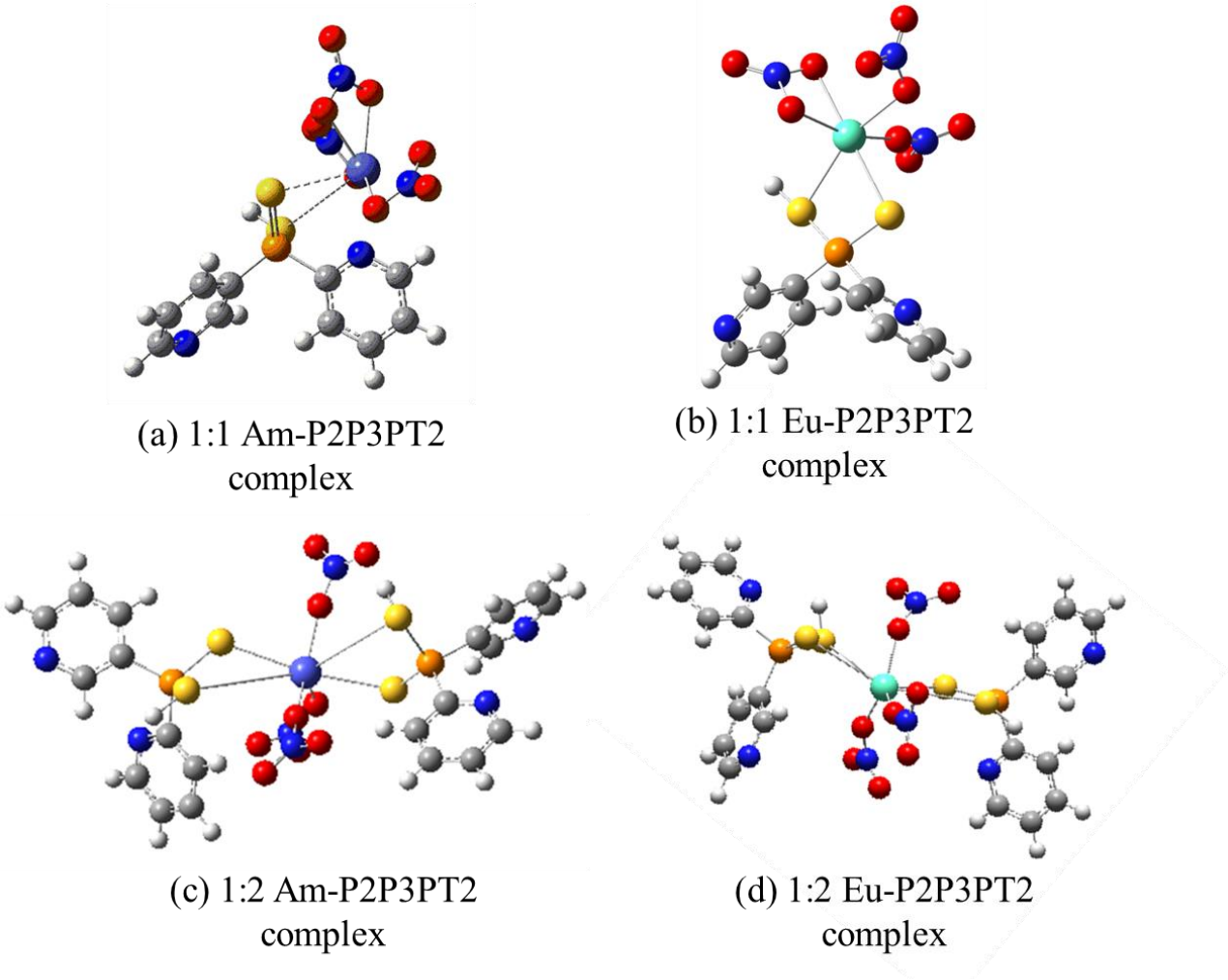

Figure 4.7 Three-dimensional optimized geometries of Am/Eu-P2P3PT2 complexes

4.2.5 Am/Eu PPPT2 Ligand complexes

According to the obtained results (Table 4.2) the formation of 1:1 Am-PPPT2 complex (Figure 4.4 a) is an exothermic reaction with -19.77 Kcal/mol energy in the gas phase (-12.74 Kcal/mol in n-dodecane solvent) relative to separate metal salt and ligand. Contrarily, the formation of 1:1 Eu-PPPT2 complex (Figure 4.4 b) is an exothermic reaction with energy -8.21 Kcal/mol (endothermic, 5.45 Kcal/mol) relative to the separate metal salt and ligand. The relative energy obtained for 1:2 Am-PPPT2 complex (Figure 4.6 c) is -16.29 Kcal/mol (-50.61 Kcal/mol) relative to the separate

metal salts and PPPT2 ligand. Similarly, the relative energy calculated for the formation of the 1:2 Eu-PPPT2 complex (Figure 4.6 d) is -43.19 Kcal/mol (-53.87 Kcal/mol).

In n-dodecane solvent:

Ratio	1:1 Am-PPPT2 → 1:2 Am-PPPT2 → 1:3 Am-PPPT2
ΔE	-12.74 Kcal/mol → -50.61 Kcal/mol → not optimized
Ratio	1:1 Eu-PPPT2 → 1:2 Eu-PPPT2 → 1:3 Eu-PPPT2
ΔE	5.45 Kcal/mol → -53.87 Kcal/mol → not optimized

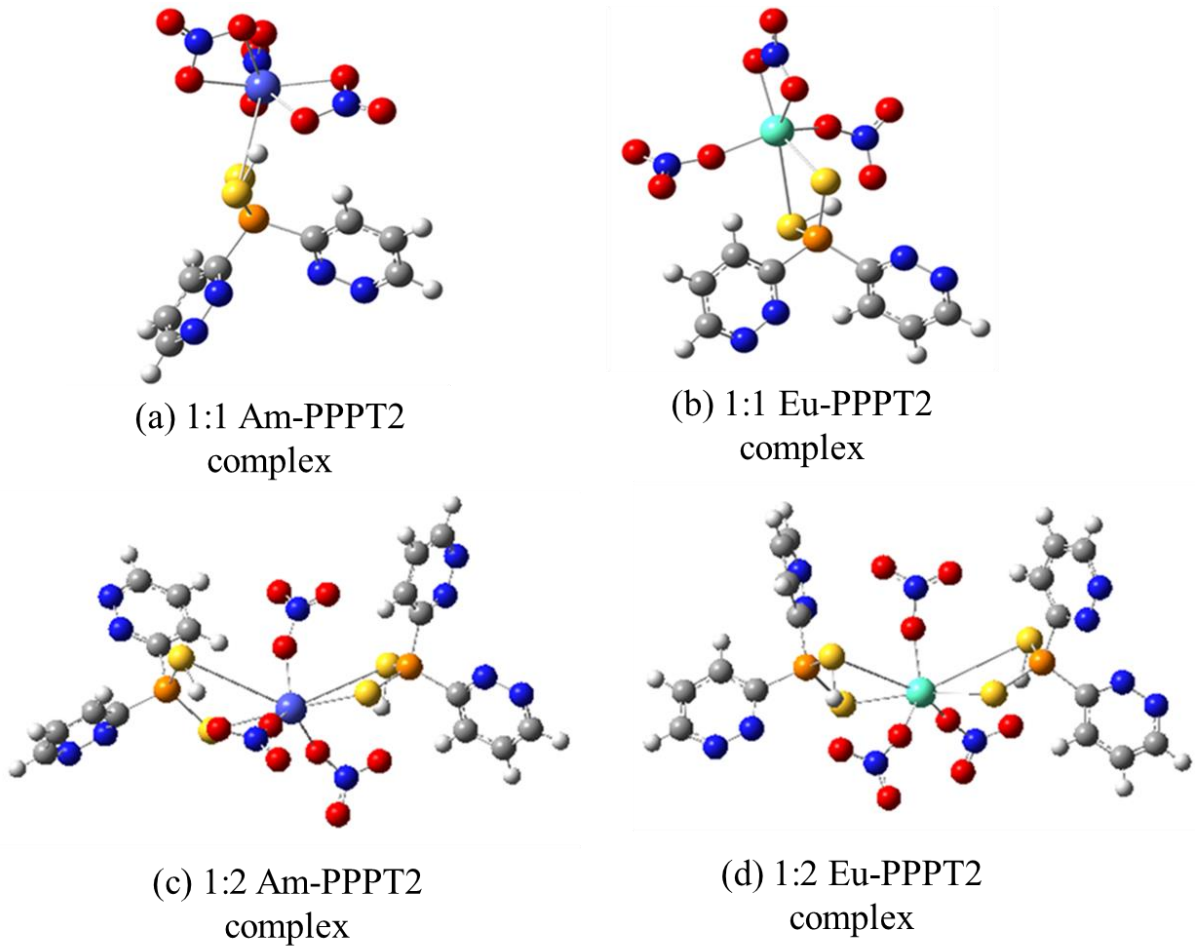

Figure 4.8 Three-dimensional optimized geometries of Am/Eu-PPPT2 complexes

DFT calculations assisted to interpret the significant differences between the relative energies of Am and Eu complexes with organo phosphinodithioic acid ligand and its derivatives

in n-dodecane solvent. According to the computational results (Table 4.2), the order of stability for 1:1 Am complexes with these ligands is Am-P2P3PT2 > Am-PPPT2 > Am-P3P3PT2 > Am-P2P2PT2 > Am-BphPT2, which clearly explain that Am forms most stable metal ligand complex with P2P3PT2 ligand in n-dodecane solvent, therefore can be best extracted with this ligand, while Am-BphPT2 exhibited a highly endothermic reaction and resulted in the generation of an unstable complex, rendering extraction of Am with BphPT2 ligand impossible.

On the other hand, computational results obtained for 1:1 Eu complexes with organo phosphinodithioic acid ligand (1:1) and its derivatives in n-dodecane solvent show the stability order of Eu-P3P3PT2 > Eu-P2P2PT2 > Eu-P2P3PT2 > Eu-PPPT2 > Eu-BphPT2, giving the most stable Eu metal complex with P3P3PT2, however the least stable complex with BphPT2 ligand, making Eu extraction with this ligand impossible. Therefore, it was deduced that Am metal can be extracted from nuclear waste using P2P3PT2 ligand, which has nitrogen atoms; one at ortho and other at meta positions of the two pyridine rings of organo phosphinodithioic acid derivative. Whereas the P3P3PT2 ligand, in which both nitrogen atoms are at the meta position of each pyridine ring, is effective for extracting Eu metal.

Now to optimize the metal to ligand ratio, models of Am/Eu complexes with two ligands each were designed. According to the relative energy data obtained, the stability of metal ligand complexes increased when the ratio was increased from 1:1 to 1:2. The order of stability for 1:2 Am complexes with these organo phosphinodithioic ligand and its derivatives is Am-BphPT2 > Am-PPPT2 > Am-P3P3PT2 > Am-P2P3PT2 > Am-P2P2PT2, whereas the order of stability for Eu-Ligand complexes is Eu-PPPT2 > Eu-P2P3PT2 > Eu-P3P3PT2 > Eu-BphPT2 > Eu-P2P2PT2 in n-dodecane solvent. Based on these findings, it was predicted that employing the 1:3 M-L ratio would further increase complex stability. For this purpose, Am/Eu complexes with all five ligands

were designed, but only one complex, Am-BphPT2, was successfully optimized. When the metal to ligand ratio of the Am-BphPT2 complex was increased from 1:2 to 1:3, the obtained result was the inverse of what was predicted, with the increased relative energy. The reason for this could be steric hindrance caused by the bulky ligand molecules. As a result, we propose that a 1:2 M-L ratio is the optimized ratio to extract the Am/Eu metals using organo phosphinodithioic acid ligands.

Concluding the overall suitability of ligands to extract the Am from Eu, computational analysis reveals that a metal to ligand ratio of 1:2 is ideal for extracting Am/Eu metals from used nuclear waste. Also, BphPT2, an organo phosphinodithioic ligand derivative, is suitable for extracting Am, whereas PPPT2 is best for extracting Eu. This also validates the Hard and Soft Acids and Basis (HSAB) concept/principle, which states that americium has a higher affinity for soft ligands containing S-donor atoms than europium.

5 Conclusion

The hazardous spent nuclear waste produced as a result of electric power generation in nuclear power plants consists of a mixture of radioactive nuclides with varying half-lives. For the safe and long-term disposal of waste, it is necessary to extract highly radioactive nuclides with longer half-lives, notably minor actinides. Separation of trivalent actinides particularly Am^{+3}, and lanthanides, i.e., Eu^{+3} is one of the most important steps in the spent nuclear fuel reprocessing. However, it is very difficult and challenging to separate them due to their similar chemical properties. In this study, DFT calculations were carried out at the energy level of B3LYP/SDD hybrid density functional to optimize all modelled geometries of the organo phosphinodithioic acid ligand and its four derivatives, as well as their complexes with Am and Eu metals in the ratios of 1:1, 1:2, and 1:3 in n-dodecane solvent. According to the obtained relative energy data, the stability of metal ligand complexes increased when the ratio was increased from 1:1 to 1:2, but it was decreased when the ratio was increased from 1:2 to 1:3 due to steric hindrance caused by the bulky ligand molecules. As a result, it is concluded that a 1:2 M-L ratio is the ideal ratio to extract the Am/Eu metals using organo phosphinodithioic acid ligands in n-dodecane solvent.

Furthermore, it is found that Am is best extracted with an organo phosphinoditjioic acid ligand derivative, benzyl(phenyl) phosphinodithioic acid (BphPT2) ligand, whereas pyridazin-3-yl(pyridazin-3-ylmethyl) phosphinodithioic acid (PPPT2) is best for extracting Eu. The studied extractants exhibit excellent extractability for Am/Eu metals and are inexpensive and

environmentally safe. However, there was one limitation encountered during this study as well. The basis sets for Eu and Am metals (4f/5f transition metals) are very heavy, so the simulation took more than a month on single simulation with 1:1 M-L ratio. With the increase of number of ligands, the simulation time was increased 3-4 times. That is the major reason that we are succeeded with the geometry optimization of only one simulation for 1:3 M-L complex.

6 Future work

This work lays the theoretical groundwork for future synthetic efforts to concentrate on the preparation of organo phosphinodithioic acid ligands and their derivates for the use in the separation of Am^{+3}/Eu^{+3} in experimental chemistry laboratories. Furthermore, the Pakistan Atomic Energy Commission (PAEC) will be presented with the idea of proposing these useful Am^{+3}/Eu^{+3} separating ligands for use in large-scale industrial nuclear fuel reprocessing. Also, it is hoped that this research will aid in the development of more effective Am^{+3}/Eu^{+3} separating ligands in the future.

References

[1] A. H. Johnstone, “CRC Handbook of Chemistry and Physics-69th Edition Editor in Chief R. C. Weast, CRC Press Inc., Boca Raton, Florida, 1988, pp. 2400, price £57.50. ISBN 0-8493-0369-5,” *J. Chem. Technol. Biotechnol.*, vol. 50, no. 2, pp. 294–295, 2007, doi: 10.1002/jctb.280500215.

[2] J. A. Rard, “Chemistry and Thermodynamics of Ruthenium and Some of Its Inorganic Compounds and Aqueous Species,” *Chem. Rev.*, vol. 86, no. 4, p. 731, 1986, doi: 10.1021/cr00074a600.

[3] M. Y. A. Yagoub, H. C. Swart, L. L. Noto, J. H. O’Connel, M. E. Lee, and E. Coetsee, “The effects of Eu-concentrations on the luminescent properties of SrF 2:Eu nanophosphor,” *J. Lumin.*, vol. 156, pp. 150–156, 2014, doi: 10.1016/j.jlumin.2014.08.014.

[4] P. Henderson, “General geochemical properties and abundances of the rare earth elements.,” *Rare Earth Elem. Geochemistry*, pp. 1–32, 1983, doi: 10.1016/b978-0-444-42148-7.50006-x.

[5] A. Ugale, T. N. Kalyani, and S. J. Dhoble, *Potential of europium and samarium β-diketonates as red light emitters in organic light-emitting diodes*. Elsevier Inc., 2018. doi: 10.1016/B978-0-12-813840-3.00002-8.

[6] *No TitleSilva, R. J., Bidoglio, G., Robouch, P. B., Puigdomenech, I., Wanner, H., & Rand, M. H. (2012). Chemical thermodynamics of americium. Newnes.*

[7] W. H. Runde and W. W. Schulz, “AMERICIUM,” 1985.

[8] W. H. Runde and B. J. Mincher, “Higher oxidation states of americium: Preparation, characterization and use for separations,” *Chem. Rev.*, vol. 111, no. 9, pp. 5723–5741, 2011, doi: 10.1021/cr100181f.

[9] A. J. Francis, *Impacts of microorganisms on radionuclides in contaminated environments and waste materials*. Woodhead Publishing Limited, 2012. doi: 10.1533/9780857097194.1.161.

[10] C. Poinssot *et al.*, “Assessment of the environmental footprint of nuclear energy systems. Comparison between closed and open fuel cycles,” *Energy*, vol. 69, pp. 199–211, 2014, doi: 10.1016/j.energy.2014.02.069.

[11] D. N. Suglobov, R. M. Yakovlev, and B. F. Myasoedov, “Thorium-uranium fuel cycle for heat and power engineering,” *Radiochemistry*, vol. 49, no. 5, pp. 441–448, 2007, doi: 10.1134/S1066362207050013.

[12] J. D. McDonald, “Nuclear waste disposal,” *Phys. Today*, vol. 29, no. 11, pp. 13–90, 1976, doi: 10.1063/1.3024493.

[13] M. Frankel, “Radioactive waste,” *Plumb. Eng.*, vol. 17, no. 3, pp. 30–32, 34, 1989, doi: 10.4324/9781315643724-16.

[14] B. Zohuri, *Nuclear fuel cycle and decommissioning*. Elsevier Ltd., 2020. doi: 10.1016/b978-0-12-818483-7.00002-0.

[15] R. Burcl, “Radioactive waste (RAW) categories, characterization and processing route selection,” *Radioact. Waste Manag. Contam. Site Clean-Up Process. Technol. Int. Exp.*, pp. 50–72, 2013, doi: 10.1533/9780857097446.1.50.

[16] W. Is and L. R. Waste, “10. What Is Low-Level Radioactive Waste?”.

[17] M. V. Ramana, “Technical and social problems of nuclear waste,” *Wiley Interdiscip. Rev. Energy Environ.*, vol. 7, no. 4, pp. 1–12, 2018, doi: 10.1002/wene.289.

[18] J. Narbutt, *Solvent extraction for nuclear power*. Elsevier Inc., 2019. doi: 10.1016/B978-0-12-816911-7.00024-4.

[19] M. I. Ojovan and W. E. Lee, “Nuclear Waste Types and Sources,” *An Introd. to Nucl. Waste Immobil.*, pp. 75–97, 2014, doi: 10.1016/b978-0-08-099392-8.00008-5.

[20] B. Kienzler and H. Geckeis, “Radioactive wastes and disposal options,” *EPJ Web Conf.*, vol. 189, 2018, doi: 10.1051/epjconf/201818900014.

[21] H. Feiveson, Z. Mian, M. Ramana, and F. Von Hippel, *Managing spent fuel from nuclear power reactors: Experience and lessons from around the world*. 2011.

[22] K. R. Rao, “Radioactive waste: The problem and its management,” *Curr. Sci.*, vol. 81, no. 12, pp. 1534–1546, 2001.

[23] M. J. Hudson, L. M. Harwood, D. M. Laventine, and F. W. Lewis, “Use of soft heterocyclic N-donor ligands to separate actinides and lanthanides,” *Inorg. Chem.*, vol. 52, no. 7, pp. 3414–3428, 2013, doi: 10.1021/ic3008848.

[24] International Atomic Energy Agency, “Status of Minor Actinide Fuel Development,” *IAEA Nucl. Energy Ser.*, pp. 1–95, 2009.

[25] J. Bruno and R. C. Ewing, “Spent nuclear fuel,” *Elements*, vol. 2, no. 6, pp. 343–349, 2006, doi: 10.2113/gselements.2.6.343.

[26] N. Belyakov, *Modern nuclear power plant*. 2019. doi: 10.1016/b978-0-12-817012-0.00024-4.

[27] Q. Zhang, Y. Jiang, X. Zhao, J. Chen, D. Xia, and B. Zhang, “Research Progress on the Corrosive Environment Large-Scale Evolution for Nuclear Waste Container,” vol. 9, no.

July, pp. 1–10, 2022, doi: 10.3389/fmats.2022.929639.

[28] J. L. Zhu and C. Y. Chan, “Radioactive waste management. World overview,” *Int. At. Energy Agency Bull.*, vol. 31, no. 4, pp. 5–13, 1989.

[29] N. Waste, “i u n s n,” 1978.

[30] A. Adamantiades and I. Kessides, “Nuclear power for sustainable development: Current status and future prospects,” *Energy Policy*, vol. 37, no. 12, pp. 5149–5166, 2009, doi: 10.1016/j.enpol.2009.07.052.

[31] M. Apted and J. Ahn, “Multiple-barrier geological repository design and operation strategies for safe disposal of radioactive materials,” *Geol. Repos. Syst. Safe Dispos. Spent Nucl. Fuels Radioact. Waste*, pp. 3–28, 2010, doi: 10.1533/9781845699789.1.3.

[32] M. Salvatores, “Nuclear fuel cycle strategies including Partitioning and Transmutation,” *Nucl. Eng. Des.*, vol. 235, no. 7, pp. 805–816, 2005, doi: 10.1016/j.nucengdes.2004.10.009.

[33] M. Riedel, A. Streit, F. Wolf, T. Lippert, and D. Kranzlmüller, “Classification of different approaches for e-science applications in next generation computing infrastructures,” *Proc. - 4th IEEE Int. Conf. eScience, eScience 2008*, no. May 2014, pp. 198–205, 2008, doi: 10.1109/eScience.2008.56.

[34] E. Shakerzadeh, *Theoretical investigations of interactions between boron nitride nanotubes and drugs*. Elsevier Inc., 2016. doi: 10.1016/B978-0-323-38945-7.00004-3.

[35] T. Henning, *Lecture Notes in Physics: Preface*, vol. 815. 2010.

[36] F. G. Becker *et al.*, “COMPUTATIONAL CHEMISTRY Introduction to the Theory and Applications of Molecular and Quantum Mechanics,” *Syria Stud.*, vol. 7, no. 1, pp. 37–72, 2015, [Online]. Available:

https://www.researchgate.net/publication/269107473_What_is_governance/link/548173090cf22525dcb61443/download%0Ahttp://www.econ.upf.edu/~reynal/Civil wars_12December2010.pdf%0Ahttps://think-asia.org/handle/11540/8282%0Ahttps://www.jstor.org/stable/41857625

[37] T. GUND, "Molecular Modeling of Small Molecules," *Guideb. Mol. Model. Drug Des.*, pp. 55–92, 1996, doi: 10.1016/b978-012178245-0/50004-4.

[38] V. J. Gillet and A. R. Leach, *Chemoinformatics*, vol. 3, no. October. Elsevier Inc., 2006. doi: 10.1016/b978-0-12-409547-2.14327-6.

[39] S. A. Hollingsworth and R. O. Dror, "Molecular Dynamics Simulation for All," *Neuron*, vol. 99, no. 6, pp. 1129–1143, 2018, doi: 10.1016/j.neuron.2018.08.011.

[40] J. B. Adams, "Bonding Energy Models," *Encycl. Mater. Sci. Technol.*, pp. 763–767, 2001, doi: 10.1016/b0-08-043152-6/00146-7.

[41] J. Kostal, *Computational Chemistry in Predictive Toxicology: status quo et quo vadis?*, 1st ed., vol. 10. Elsevier B.V., 2016. doi: 10.1016/B978-0-12-804700-2.00004-0.

[42] F. J. Heldrich *et al.*, *Computational chemistry*. 2004. doi: 10.1201/b16812-34.

[43] K. I. Ramachandran, G. Deepa, and K. Namboori, "Computational chemistry and molecular modeling: Principles and applications," *Comput. Chem. Mol. Model. Princ. Appl.*, pp. 1–397, 2008, doi: 10.1007/978-3-540-77304-7.

[44] A. C. Tsipis, "DFT flavor of coordination chemistry," *Coord. Chem. Rev.*, vol. 272, pp. 1–29, 2014, doi: 10.1016/j.ccr.2014.02.023.

[45] A. P. Paiva and P. Malik, "Recent advances on the chemistry of solvent extraction applied to the reprocessing of spent nuclear fuels and radioactive wastes," *J. Radioanal. Nucl. Chem.*, vol. 261, no. 2, pp. 485–496, 2004, doi: 10.1023/B:JRNC.0000034890.23325.b5.

[46] C. E. I. C. Whipple, "'Disposal of Spent nuclear fuel and high-level radioactive waste.,'" 2010.

[47] J. S. Stuckless and R. A. Levich, "The road to Yucca Mountain - Evolution of nuclear waste disposal in the United States," *Environ. Eng. Geosci.*, vol. 22, no. 1, pp. 1–25, 2016, doi: 10.2113/gseegeosci.22.1.1'.

[48] I. G. McKinley, W. Russell Alexander, and P. C. Blaser, "Development of geological disposal concepts," *Radioact. Environ.*, vol. 9, no. 06, pp. 41–76, 2007, doi: 10.1016/S1569-4860(06)09003-6.

[49] T. R. Society, P. Transactions, R. Society, and P. Sciences, "Available options for waste disposal".

[50] International Atomic Energy Agency, *Assessment of Partitioning Processes for Transmutation of Actinides*. 2010.

[51] G. Modolo, A. Wilden, P. Kaufholz, D. Bosbach, and A. Geist, "Development and demonstration of innovative partitioning processes (i-SANEX and 1-cycle SANEX) for actinide partitioning," *Prog. Nucl. Energy*, vol. 72, pp. 107–114, 2014, doi: 10.1016/j.pnucene.2013.07.021.

[52] Y. Wei, R. Liu, Y. Wu, J. Zu, X. Wang, and Z. Chen, "Chromatographic separation of actinides and fission products," *Energy Procedia*, vol. 39, pp. 110–119, 2013, doi: 10.1016/j.egypro.2013.07.197.

[53] K. L. Nash and G. R. Choppin, "Separations chemistry for actinide elements: Recent developments and historical perspective," *Sep. Sci. Technol.*, vol. 32, no. 1–4, pp. 255–274, 1997, doi: 10.1080/01496399708003198.

[54] S. A. Ansari, P. K. Mohapatra, and V. K. Manchanda, "Recovery of actinides and

lanthanides from high-level waste using hollow-fiber supported liquid membrane with TODGA as the carrier," *Ind. Eng. Chem. Res.*, vol. 48, no. 18, pp. 8605–8612, 2009, doi: 10.1021/ie900265y.

[55] E. H. K. Aneheim, "Development of a Solvent Extraction Process for Group Actinide Recovery from Used Nuclear Fuel," *Dept. Chem. Biol. Eng.*, vol. Ph.D., p. 90, 2012.

[56] A. Leoncini, J. Huskens, and W. Verboom, "Ligands for f-element extraction used in the nuclear fuel cycle," *Chem. Soc. Rev.*, vol. 46, no. 23, pp. 7229–7273, 2017, doi: 10.1039/c7cs00574a.

[57] J. N. Mathur, M. S. Murali, and K. L. Nash, "Actinide partitioning-A review," *Solvent Extr. Ion Exch.*, vol. 19, no. 3, pp. 357–390, 2001, doi: 10.1081/SEI-100103276.

[58] B. C. Na and E. Sartori, "Organization for economic cooperation and development/nuclear energy agency international benchmark on the VENUS-2 MOX core measurements," *Nucl. Sci. Eng.*, vol. 142, no. 1, pp. 37–47, 2002, doi: 10.13182/NSE02-A2285.

[59] M. Nilsson and K. L. Nash, "Review article: A review of the development and operational characteristics of the TALSPEAK process," *Solvent Extr. Ion Exch.*, vol. 25, no. 6, pp. 665–701, 2007, doi: 10.1080/07366290701634636.

[60] E. H. K. Aneheim, *Development of a Solvent Extraction Process for Group Actinide Recovery from Used Nuclear Fuel*, vol. Ph.D. 2012.

[61] C. Anderson, H. H., Newton, Mass, Asprey, L. B., Richmond, "No TitleSolvent extraction process for plutonium," 1960. [Online]. Available: https://scholar.google.com/scholar?hl=en&as_sdt=0%252C5&q=Anderson%252C+H.+H.%252C+Newton%252C+Mass%252C+Asprey%252C+L.+B.%252C+Richmond%252C+Calif.+Solvent++extraction+process+for+plutonium%252C+United+States+Patent+Offic

e%252C+patent+no+2%252C924%252C506.++Applied+08-05-1947%252

[62] J. Veliscek-Carolan, “Separation of actinides from spent nuclear fuel: A review,” *J. Hazard. Mater.*, vol. 318, pp. 266–281, 2016, doi: 10.1016/j.jhazmat.2016.07.027.

[63] S. K. Sood, D. D., & Patil, “Chemistry of nuclear fuel reprocessing: current status.,” *J. Radioanal. Nucl. Chem.*, pp. 547–573, 1996.

[64] G. De Roo and J. E. Parsons, “A methodology for calculating the levelized cost of electricity in nuclear power systems with fuel recycling,” *Energy Econ.*, vol. 33, no. 5, pp. 826–839, 2011, doi: 10.1016/j.eneco.2011.01.008.

[65] Nea, *Potential Benefits and Impacts of Advanced Nuclear Fuel Cycles with Actinide Partitioning and Transmutation*, vol. 6894, no. m. 2011.

[66] C. Madic, M. Lecomte, P. Baron, and B. Boullis, “Separation of long-lived radionuclides from high active nuclear waste,” *Comptes Rendus Phys.*, vol. 3, no. 7–8, pp. 797–811, 2002, doi: 10.1016/S1631-0705(02)01370-1.

[67] I. May, R. J. Taylor, G. C. Brown, and N. J. Hill, “Np(IV) Distribution between 30% Tributylphosphate in Odourless Kerosene and Nitric Acid,” *Radiochim. Acta*, vol. 83, no. 3, pp. 135–138, 1998, doi: 10.1524/ract.1998.83.3.135.

[68] K. L. Nash, “Chapter 121 Separation chemistry for lanthanides and trivalent actinides,” *Handb. Phys. Chem. Rare Earths*, vol. 18, pp. 197–238, 1994, doi: 10.1016/S0168-1273(05)80044-3.

[69] K. L. Nash, C. Madic, J. N. Mathur, and J. Lacquement, “Actinide Separation Science and Technology,” *Chem. Actin. Trans. Elem.*, pp. 2622–2798, 2010, doi: 10.1007/978-94-007-0211-0_24.

[70] E. P. Horwitz, W. W. Schulz, and C. Division, “THE TRUEX PROCESS : A VITAL

TOOL FOR," no. Iii, pp. 21–29, 1991.

[71] O. Courson *et al.*, "Separation of Minor Actinides from Genuine HLLW Using the DIAMEX Process," *5th Int. Inf. Exch. Meet. Mol.*, pp. 1–10, 1998.

[72] Kok, Kenneth D., ed. Nuclear engineering handbook. CRC Press, 2016.

[73] G. Modolo, A. Wilden, A. Geist, D. Magnusson, and R. Malmbeck, "A review of the demonstration of innovative solvent extraction processes for the recovery of trivalent minor actinides from PUREX raffinate," *Radiochim. Acta*, vol. 100, no. 8–9, pp. 715–725, 2012, doi: 10.1524/ract.2012.1962.

[74] J. Westwood and L. M. Harwood, "Controlling Actinide Extraction Chemistry (Separation of Actinides from Lanthanides as Part of Nuclear Fuel Recycling)," *Encycl. Inorg. Bioinorg. Chem.*, pp. 1–17, 2018, doi: 10.1002/9781119951438.eibc2529.

[75] T. Guoxin *et al.*, "Investigation of the extraction complexes of light lanthanides(III) with bis(2,4,4-trimethylpentyl)dithiophosphinic acid by EXAFS, IR, and MS in comparison with the americium(III) complex," *Inorg. Chem.*, vol. 42, no. 3, pp. 735–741, 2003, doi: 10.1021/ic025783z.

[76] K. L. Nash, "Solvent Extraction and Ion Exchange The Chemistry of TALSPEAK : A Review of the Science," no. January, pp. 37–41, 2015.

[77] C. Musikas, "IRDI-DERDCA-DPR~SE -SCPR Centre d'Etudes Nucléaires de Fontenay-Aux-Roses BP n° 6 - Fontenay-Aux-Roses - France," pp. 16–21, 1984.

[78] "'.aLio^ul mj^tin of th_ . >r:crican C!v;-~..i.:ji 5oji.t>. HwP.olè'j !c;',:-ii, l-é.V.-ii '979 : 3".

[79] H. H. Dam, D. N. Reinhoudt, and W. Verboom, "Multicoordinate ligands for actinide/lanthanide separations," *Chem. Soc. Rev.*, vol. 36, no. 2, pp. 367–377, 2007, doi:

10.1039/b603847f.

[80] Y. Zhu, “The Separation of Americium from Light Lanthanides by Cyanex 301 Extraction,” *Radiochim. Acta*, vol. 68, no. 2, pp. 95–98, 1995, doi: 10.1524/ract.1995.68.2.95.

[81] Y. Zhu, J. Chen, and R. Jiao, “Solvent Extraction and Ion Exchange Extraction of Am (III) and Eu (III) from Nitrate Solution with Purified Cyanex 301,” no. May 2013, pp. 37–41, 2007.

[82] “membranes containing cyanex 301.”

[83] Z. Lovasic, “Spent Fuel Reprocessing Options,” *Nucl. Fuel Cycle Mater. Sect.*, no. August, p. 151, 2008.

[84] J. Chen, R. Jiao, and Y. Zhu, “A study on the radiolytic stability of commercial and purified Cyanex 301,” *Solvent Extr. Ion Exch.*, vol. 14, no. 4, pp. 555–565, 1996, doi: 10.1080/07366299608918356.

[85] C. A. Sharrad and D. M. Whittaker, *The use of organic extractants in solvent extraction processes in the partitioning of spent nuclear fuels*. Elsevier Ltd., 2015. doi: 10.1016/B978-1-78242-212-9.00007-1.

[86] P. Taylor *et al.*, “Solvent Extraction and Ion Exchange Agent for the Separation of Americium (III) and Curium (III) from the Lanthanides,” no. September 2012, pp. 37–41, 2007, doi: 10.1080/07366290600761936.

[87] D. Magnusson *et al.*, “Demonstration of a SANEX process in centrifugal contactors using the CyMe4-BTBP molecule on a genuine fuel solution,” *Solvent Extr. Ion Exch.*, vol. 27, no. 2, pp. 97–106, 2009, doi: 10.1080/07366290802672204.

[88] G. C. Dugoni, E. Mossini, E. Macerata, A. Sacchetti, A. Mele, and M. Mariani, “Deep

Eutectic Solvents : Promising Co-solvents to Improve the Extraction Kinetics of CyMe 4 - BTBP," 2021, doi: 10.1021/acsomega.0c05109.

[89] L. M. Harwood, F. W. Lewis, J. Hudson, J. John, and P. Distler, "Solvent Extraction and Ion Exchange The Separation of Americium (III) from Europium (III) by Two New 6 , 6 ' - Different Diluents," no. September 2012, pp. 551–576, 2011.

[90] D. Dubbeldam, J. Vreede, T. J. Vlugt, and S. Calero, "Highlights of (bio-)chemical tools and visualization software for computational science," *Curr. Opin. Chem. Eng.*, vol. 23, pp. 1–13, 2019, doi: 10.1016/j.coche.2019.02.001.

[91] L. Radom, "John A. Pople (1925–2004)," *Nature*, vol. 428, no. 6985, pp. 816–816, 2004, doi: 10.1038/428816a.

[92] D. Zhou and H. Kong, *Encyclopedia of Applied and Computational Mathematics*, no. 2. 2015. doi: 10.1007/978-3-540-70529-1.

[93] A. Manuscript, "www.rsc.org/njc".

[94] G. Schaftenaar and J. H. Noordik, "Molden: A pre- and post-processing program for molecular and electronic structures," *J. Comput. Aided. Mol. Des.*, vol. 14, no. 2, pp. 123–134, 2000, doi: 10.1023/A:1008193805436.